Research Square

Preprints are preliminary reports that have not undergone peer review.
They should not be considered conclusive, used to inform clinical practice,
or referenced by the media as validated information.

Predicting the process parameters for torque and thrust force in wood plastic composite drilling using machine learning algorithms

Palanikumar Kayaroganam

palanikumar_k@yahoo.com

Sri Sai Ram Engineering College

Sundarapandiyan Murugesan

Sri Sai Ram Engineering College

Sreedevi B

Sri Sai Ram Engineering College

Latha Balasubramanian

Sri Sai Ram Engineering College

Research Article

Keywords: Wood plastic composites, Machine learning, Drilling, Thrust force, Torque, Key performance indicator

Posted Date: September 4th, 2026

DOI: https://doi.org/10.21203/rs.3.rs-10625201/v1

License: This work is licensed under a Creative Commons Attribution 4.0 International License.
Read Full License

Additional Declarations: No competing interests reported.

Predicting the process parameters for torque and thrust force in wood plastic composite drilling using machine learning algorithms

Palanikumar Kayaroganam*

Department of Mechanical Engineering,

Sri Sai Ram Engineering College, Chennai-600 044, India

* Correspondence: palanikumar_k@yahoo.com

Tel.: 9677053338

Sundarapandiyan Murugesan

Department of Mechanical Engineering,

Sri Sai Ram Engineering College, Chennai-600 044, India

murusundarm@gmail.com

Mrs. Sreedevi B

Department of Computer Science and Engineering,

Sri Sai Ram Institute of Technology, Chennai-600 044, India.

hodcse@sairamit.edu.in

Mrs. Latha Balasubramanian

Department of Computer Science and Engineering,

Sri Sai Ram Engineering College, Chennai-600 044, India

sivasoorya2003@yahoo.com

Abstract

Wood Plastic Composite has become increasingly notable in domestic and industrial applications. The excessive thrust force and torque generated during drilling lead to poor surface finish and potential damage to the work materials. The drilling experiments were performed using Taguchi's L_{27} orthogonal array, with drilling parameters (*N, f,* and *d*) as inputs and thrust force and torque as output responses. The ANOVA analysis reveals that feed rate contributes (65.16% for thrust force and 64.41% for torque), followed by drill diameter (27.33% for thrust force and 20.39% for torque), and spindle speed (4.90% for thrust force and 12.84% for torque). Furthermore, machine learning models such as the extra-trees regressor, bagging with decision trees, and the random forest regressor were built to predict the output responses of WPC composite panels. To evaluate the performance of the predicted outcomes, six error metrics were used: mean absolute percentage error, mean absolute difference, Root mean square error, Standard error, mean square error, and coefficient of determination. Compared with other models, random forest produces more accurate predictions for thrust force and torque. This study provides a novel approach for evaluating and identifying suitable process parameters to minimize thrust force and torque induced during drilling of WPC composites.

Keywords: Wood plastic composites, Machine learning, Drilling, Thrust force, Torque, Key performance indicator.

Nomenclature

ANFIS – Adaptive Neuro-Fuzzy Interference System

AI – Artificial Intelligence

ANOVA – Analysis of Variance

CNC- Computer Numerical Control

DD – Drill Diameter

ELM – Extreme Learn Machine

FFNN – Feed Forward Neural Network

FR – Feed Rate

F_z – Thrust Force

F_t – Torque

GPR – Gaussian Process Regression

HSS -High Speed Steel

KPI – Key Performance Indicator

LVQ – Learning Vector Quantization

ML - Machine Learning

MSE – Mean Squared Error

MAE – Mean Absolute Error

MAPE – Mean Absolute Percentage Error

MLP – Multi Layer Perception

MLP – Multi Layer Perception

R^2 – Coefficient of Correlation

RMSE – Root Mean Square Error

SS - Spindle Speed

SVM – Support Vector Machine

WPC – Wood Plastic Composite

XGBoost – Extreme Gradient Boosting

1. Introduction

Wood has been used as a structural material in various fields since ancient times, ever since humans discovered its potential applications[1]. Wood is considered a complex material that can be used for many purposes due to its anisotropic, biological nature and excellent mechanical properties. It can be used for energy conversion, wastewater purification, solar desalination, thermal insulation, structural purposes, and more[2]The lack of plantations, governmental restrictions on local trade, international trade in wood, deforestation, and the use of wood to produce charcoal force researchers to seek alternatives to wood composite materials. [3];[4]. Products that have been developed as alternatives to wood in recent years include Oriented Strand Board, Parallel-Strand Lumber, wafer board, particle board, Medium Density Fibreboard, hardboard, Wood Plastic Composite ,wood cement composite, pulp for paper, and paperboard [5]. Wood composites have gained popularity in recent years as a superior alternative to solid wood. Numerous advantages make them a top choice for various applications in construction, furniture manufacturing, and other industries due to their durability, consistency, eco-friendliness, versatility, and cost-effectiveness[6]**.** Among the various wood composite materials, Wood Plastic Composite (WPC) has gained more popularity than the others, especially after 2007, due to its excellent properties, including durability, processing performance, mechanical properties, physical properties, environmental protection, and Aesthetics.WPC is an environmentally friendly, 100% recyclable product.[7].WPC is a combination of natural wood fibres (wood flour, bamboo flour, hemp fibres, and crop stalks), thermoplastic (polyethylene, polypropylene, polyvinyl chloride, etc), and an appropriate amount of additives (coupling agents, antioxidants, flame retardants, etc) [8], [9], [10]The application of WPC has been widespread in automotive interiors, doors and windows, flooring, landscaping, decking, cladding, paneling, fencing, and furniture[11 -15] WPC has reached approximately USD 417.00 million in 2024 and is expected to reach USD 867.4 million in 2030 in the Indian market. As WPCs have large applications in various fields of engineering, to utilize them in real-world applications, they should be machined by numerous processes like sawing, milling, drilling, deep routing, and edge finishing[16].

Drilling is a common machining operation in wood composite materials, among various other machining operations, to produce holes of high quality in a composite material when connecting it to other components, including rivets, fasteners, and bolts

[17]. Usually, when drilling wood composite materials, defects include delamination, roughness, fiber pull-out, micro-cracking, matrix burning, chipping, and spalling [18]. These defects are caused by the anisotropic and layered structure of wood composite materials. Defects such as delamination are especially concerning. For example, during the final assembly of airplanes, delamination caused by the drilling process accounts for around 60% of all component rejections [19], [20]. Such damage to the wood composite material can affect the product's finish, ultimately impacting its final performance, appearance, and surface quality. The hole quality during drilling operations is influenced by several elements, including the workpiece material, cutting conditions, drill tool geometry, and tool material[21]. The twist drill and brad point drill are common types of drill used for drilling wood composite material with a special coating for wood composite material[22], [23].

Two quality indicators that impact the strength and quality of composite materials are delamination and Ra. While R_a is caused by excessive amounts of F_t and FR during drilling, delamination in the composite material is caused by excessive amounts of F_z.[24]. Delamination, Ra, and other quality parameters of the hole are important factors that could improve the efficiency of mechanical joining of wood composite materials. The proper selection of drill bit material and optimization of input parameters could improve the quality indicators of the composite material. Numerous studies examining wood-composite materials have been published. Slamani et al. (2024) investigated the impact of drill material on the hole quality of a hybrid composite using three distinct drill materials: HSS, HSS-Co5, and a solid carbide drill bit that could produce the fewest delaminations, circularity, and cylindricity errors [25]. Bedelean et al. (2024) have optimized the drilling parameters for particle board, MDF, and plywood composite materials, and the dominant parameters for delamination are the material type, F_z, and F_t [26]. In order to ascertain the impact of cutting parameters on hole circularity, Kumar et al. (2023) examined the drilling parameters of Sabai grass-reinforced composite and concluded that FR and SS are the significant elements. [27]. The F_z, F_t, and R_a developed during drilling of wood composites are strongly influenced by the point angle and FR[28], [29]. Elhadi et al. (2025) examined the FR and SS of dry drilling using solid carbide, HSS, and HSS-Co5 to ascertain the impact on chip formation and hole quality. Shorter, broken chips are formed at a lower SS and a higher FR, according to the research [30]. Palanikumar et al. (2016) further

stated that the right drill geometry design can result in better performance. It is possible to decrease F_z, F_t, and R_a by changing the drill bit's tip angle[31].

Researchers are currently using artificial intelligence to simulate machining conditions in the manufacturing sector. In this study, machine learning is used to model machining parameters. This section outlines the machine learning methodology and reviews the literature on the development of machine learning models across various manufacturing engineering domains.

A subfield of AI called machine learning (ML) creates statistical models and algorithms that allow computers to carry out tasks without explicit programming by identifying patterns in data [32]. Machine learning (ML) uses datasets to train models to generate predictions or judgments in order to enhance performance through experience rather than predefined rules [33]. By enabling the handling of complex, high-dimensional data that would be impossible for human-engineered solutions, the paradigm shift from conventional rule-based programming to data-driven learning has transformed numerous industries[34]

Machine learning, according to Arthur Samuel (1959), is a field of study that allows computers to learn without explicit programming [35]. This is expanded in contemporary interpretations to include techniques where algorithms iteratively modify settings to optimize accuracy or minimize errors on unseen data [36]. Supervised learning, unsupervised learning, reinforcement learning, and semi-supervised learning are the four primary types of machine learning [37][38]

Model selection, training, evaluation, deployment, feature engineering, and data preparation are all essential elements of machine learning [39] .ML algorithms can range from basic linear models to sophisticated neural networks and ensemble techniques.[40]. For instance, supervised learning often employs regression for continuous predictions or classification for discrete labels, while unsupervised techniques like clustering group similar data points [41]. Multi-layered neural networks, which have grown in popularity, are used in deep learning, a machine learning paradigm that enhances their ability to handle unstructured inputs such as text and images.[42];[43].

The theoretical foundations of ML are derived from computer science, statistics, and optimization; key issues include underfitting (inadequate learning from data) and overfitting (where the model performs well on training data but not on new data) [44].

These issues are addressed using cross-validation and regularization strategies [45]. The metrics used in practice are accuracy, mean Squared Error, mean absolute error, mean absolute percentage Error, coefficient of correlation, and root mean square error [46]

ML has applications in many sectors, including manufacturing (predictive maintenance), healthcare (disease prediction), and finance (fraud detection) [47], [48]. Recent developments highlight the consideration of ethical concerns, interpretability, and robustness in any open context, and/or when performing in adaptive conditions or when data distributions shift [49], [50]. ML continues to develop and combine with big data and big computing [51], [52]

Hua et al. (2025) developed ML model to predict the thermomechanical behavior of wood plastic composite[53]. The authors created the models by relating the dynamic thermomechanical attributes obtained through a 3-point bending test. They compared the ELM to other machine learning models, such as SVM, RF, BP neural network, and PSO-BP neural network. Compared to other models, ELM outperformed in terms of higher prediction accuracy and data fitting, achieving an R^2 of 0.982, a MAE of 1.363, and an RMSE of 3.311.

Vignesh et al. (2025) developed a multi-output RF regression model with hyperparameter tuning to predict F_z, F_t, and F_d in a CNC vertical machining center for CNT-filled GFRP composite[54]. The model was created by establishing the relationship between input process parameters, such as SS, FR, and filler percentage, and the output process parameters. Out of 27 experimental samples, 20 were used for training and 7 for testing data. The model achieves 98% accuracy on the training data and 3% on the testing data, indicating overfitting due to the small dataset. Zhang et al. (2025) developed an ANN model to predict fatigue life responses under multiple defects (delamination, tearing, and scratches on the hole wall). The ANN model was built using the experimental dataset. The hyperparameters, namely, hidden layer 1 (20 neurons) and hidden layer 2 (10 neurons), were used to develop the model for predicting fatigue life. The model took 50 epochs to reach a MAPE of 1.263% and an R^2 of 0.913. The final architecture comprises a 4-20-10-1 structure, with four input features (delamination factor, tearing factor, surface roughness, and width difference), two hidden layers with 20 and 10 neurons, respectively, and a single output neuron for

fatigue life[55]. Biruk et al. (2023) used a variety of machine learning algorithms. When drilling GFRP composite, drilling parameters (SS and FR), cutting force, and delamination are developed using various regression models. These algorithms are trained by relating F_z to delamination using the Kistler dynamometer and the Keyence VHX-5000 optical microscope. The Gradient Boosting Regressor outperforms the other machine learning models, achieving an R^2 of 0.948, an MAE of 6.13, and an RMSE of 8.46 [56].

Akdulum et al. (2023) proposed a model to predict F_z in the drilling of aluminum alloy using a U drill, by employing various machine learning techniques such as FFNN, GPR, SVM, XGBoost, and hybrid models like GPR+FFNN, GPR+SVM, SVM+FFNN, XGBoost+FFNN, XGBoost+GPR, XGBoost+SVM, and XGBoost+GPR+SVM+FNN. The proposed model associates the material's chemical and mechanical properties with the F_z developed during the process. The hybrid models XGBoost + FFNN and XGBoost + GPR performed best, showing high R^2 values and low prediction errors[57]. Dedeakayogullari et al. (2022) developed an ANN model (MLP, LVQ) to predict the R_a of SLM-Ti6Al4V material based on features extracted from piezoelectric sensor signals. The ANN models (MLP and LVQ) achieved 99.9% accuracy, surpassing the ANFIS model[58]. Lee et al. (2025) developed an ENN model to determine the surface quality of a hole and the cutting tool condition during robotic drilling of an Hexcel IM7 carbon fiber-reinforced Hex Ply 8552 epoxy composite material. The model is constructed by mapping the robotic drilling parameters and the servo motor torque sensor's features (fixed beneath the workpiece) to measured hole quality and tool condition. The ANN architecture is characterized by 4-13-11-1. The model resulted in 100% prediction accuracy[59].

In summary, ML is a disruptive mechanism for solving problems that permits systems to generalize from examples and respond to new observations [60], [61] .ML is interdisciplinary in nature, which warrants continued research to address issues such as data bias and expensive computations [61]

A careful review of past research shows that there are few ML models for predicting Fz and torque Ft. Surprisingly, only a limited amount of research has examined forecasting these parameters during drilling in wood-plastic composites (WPC). F_z and F_t need to be forecast when machining wood and wood composites, as

these materials are used in a variety of applications, including automotive interiors, doors and windows, flooring, landscaping, decking, cladding, paneling, fencing, and furniture. Developing an accurate machine learning-based forecasting model will help improve production efficiency, optimize resources, and enhance the impact on industrial productivity.

The present research investigates an ML-based approach to predicting F_z and F_t in a CNC vertical machining center. In the previous study by the authors [23], they have used box-Behnken experimental design and used response surface methodology and Binary Whale Optimization Algorithm (BWOA) for modeling and optimization. The current study focuses on developing a machine learning model to accurately predict F_z and F_t using data generated during the drilling process. The experiments are conducted by using L_{27} orthogonal array. The performance of the developed model was calculated and evaluated using several assessment criteria. When modeling techniques are adopted for various aspects of drilling operations, their application to predicting F_z and F_t in drilling WPC composites requires further exploration. A single-point measurement might only cover a portion of the wellbore. A continuous predictive model that can deliver real-time data on Fz and Ft is therefore crucial. In this study, the aim is to estimate the Fz and Ft induced during the drilling of a WPC composite panel board made of carbon steel with an aluminum finish, using a machine learning algorithm that takes cutting parameters as input. The popular machine learning techniques, such as Extra Tree regressor, bagging with decision trees, and random forest regressor, were employed to predict the Fz and Ft induced during drilling of WPC composite, as well as to build a machine learning model that takes into consideration the cutting parameters.

2. Materials and Measurements

2.1 Machining experiment and Measurement

In recent years, Wood Plastic Composite (WPC) materials have become popular for use in applications including decks, fencing, wall panels, and furniture due to their appearance, corrosion resistance, and lower weight than wood. The properties of the WPC composite being studied are presented in Table 1. Drilling is essential for creating holes in WPC materials for the assembly of components. The key factors affecting the performance of drilling wood-composite materials are SS, FR, and DD. The input

parameters for drilling WPC composite materials are selected based on a preliminary study[62] [63], [64]. The experimental limits for this investigation have been selected after a detailed analysis. Based on this analysis, the limits are as follows:

i. From existing studies, it is indicated that F_z rises with lower N and declines with higher N[65]. This happens because the cutting force increases at lower speeds. A better surface finish and minimum F_z occur at higher speeds. Typically, SS is chosen between 1000 and 3000 rpm.

ii. From existing studies, it is indicated that an increase in FR results in a higher F_z, which in turn leads to more delamination and surface damage. Conversely, a lower FR contributes to a reduced F_z, leading to smooth drilling and better quality[66]. Typically, FR is chosen between 75mm/min and 225mm/min.

iii. The DD had a considerable effect on F_z, F_t, delamination, and the overall quality of holes in NFRPCs. The larger diameter during drilling increases material removal resistance, which in turn can cause fiber pullout, matrix cracking, and surface irregularity. Whereas a small diameter tends to produce a cleaner hole with minimal delamination and a better surface finish[67]. Therefore, in this investigation, the DD was chosen between 6 and 10mm. The experimental factors and their nomenclature are shown in Table 2.

Table 1

WPC wood composites' constituents

WPC Material Composition		
Wood Fibers (40%)	Thermoplastics (54%)	Additives: Colour pigments, UV stabilizers, and antifungal agents (6%)

Table 2

The levels and their values of input process parameters

Input parameter	
Spindle speed(*N*)	1000-3000 rpm
Feed rate (*f*)	75-225 mm/min
Drill diameter(*d*)	6-10 mm

The CNC vertical machining Centre, model BMV40T20, made by Bharath Fritz Verneer, has an SS range of 60-6000 rpm. It is equipped with a Kistler multi-component dynamometer, model 9277B, and a charge amplifier, model 5070A. The

Kistler multicomponent dynamometer was calibrated in accordance with ISO 376 for F^z measurement and DIN 51309 for F_t measurement. The uncertainty in both F_z and F_t measurements was within ±1%, which is acceptable for machining experiments. The scheme of the investigation is illustrated in Fig. 1. In the present investigation, drilling experiments are performed using a brad Centre point drill bit (carbon steel with an aluminium finish), with a point angle of 118º, flute type -spiral 2 flute, rake angle of 25º, diameters of 6,8 and 10 mm, is used for investigation. Since WPC is a lightweight material compared to other wood composite materials, carbon steel with an aluminium finish could enhance the quality of the hole more than the uncoated drill bit. Fig. 2 depicts the experimental setup for creating a hole in the WPC composite using drill bits.

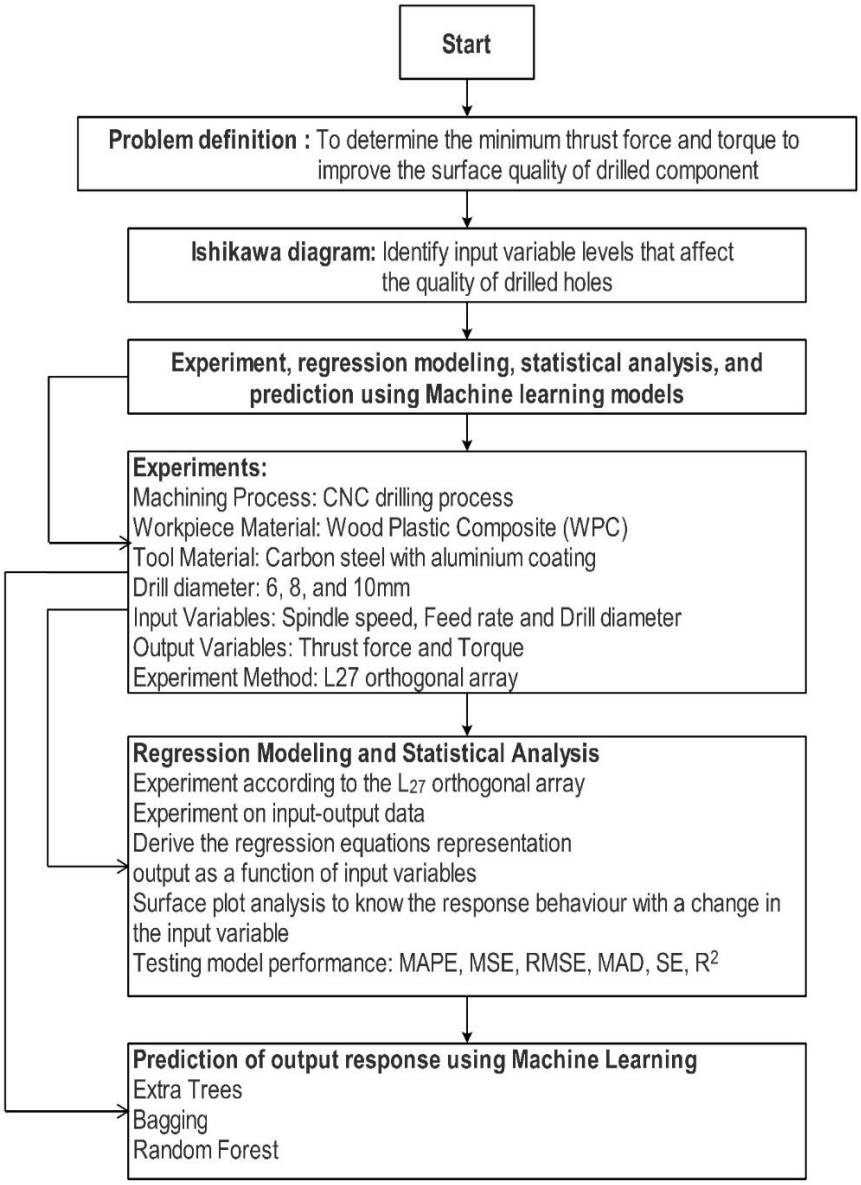


Fig. 1. Methodology used for conducting the experiment and analysis.

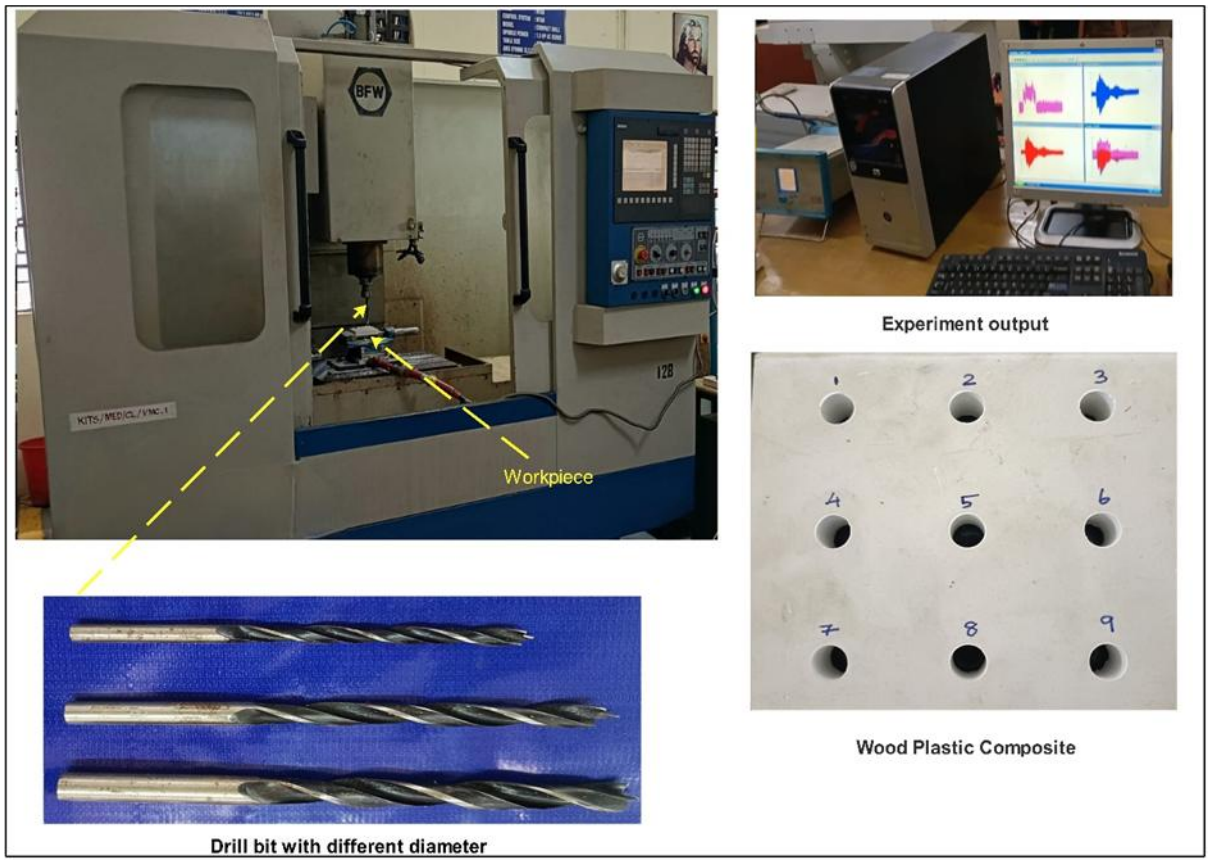


Fig. 2. Experimental setup of the drilling process

This study used a WPC composite panel purchased from EVERWOOD India; the manufacturer has not disclosed the exact formulation details, such as the species of wood fiber or the type of thermoplastic matrix, because they are proprietary. Still, the supplier's technical information states that the WPC panels are made of about 40 wt.% wood fibers, 54 wt.% thermoplastic matrix, and 6 wt.% additives, which include colour pigments, UV stabilizers, and antifungal agents. It was cut to dimensions of 100mm x 100mm x 17mm to fit within the Kistler dynamometer setup, which measures the F_z and F_t generated during drilling. The L_{27} Taguchi orthogonal array is used to design the tests, which are conducted on the CNC vertical machining center. The experiments followed the design outlined in Table 3, with 27 experiments. To ensure reliability and reduce random error during the measurement of cutting force, experiments were performed three times under dry conditions (27 x 3 = 81) to improve the statistical validity of the result. Using cooling or lubrication methods like compressed air, MQL, or mist cooling can improve quality. However, these methods

may also cause swelling or moisture absorption in wood-based fibers, which are naturally hydrophilic. This can affect their dimensional stability.

2.2 Data setting and preprocessing

The dataset includes 27 experiments, each with three trials, resulting in a total of 81 drilling tests on WPC composite panels. Each experiment recorded process parameters and their outcomes. The output variables measured were F_z and F_t. This dataset, with its 81 results, was chosen to ensure reliable predictions. No missing values were found, and all variables were standardized as needed to avoid bias from differences in scale. The data set generated during the drilling process is split into training (70%) and testing (30%) sets to assess the developed model's performance.

2.3 Development of machine learning models

2.3.1 Machine Learning Algorithms Employed

This section details the three ensemble algorithms employed in the project: Extra Trees, Bagging with Decision Trees (DT), and Random Forest. These are tree-based methods, particularly effective for regression tasks, as seen when predicting continuous outputs such as Fz and Ft. To increase accuracy and reduce variability, each algorithm constructs several decision trees and averages their predictions.

2.3.2 Extra Trees Regressor

An ensemble learning technique called Extra Trees (Extremely Randomized Trees) builds on the ideas of decision trees by adding more randomness to improve generalization and lower variance. Developed by Geurts et al. in 2006, it builds multiple unpruned decision trees from the whole data set, unlike Random Forests, which are not optimized by randomly selecting feature subsets and threshold splits. This additional randomization results in faster training times and often leads to better performance on noisy data, as it mitigates overfitting by averaging predictions across diverse trees.

In regression tasks, such as predicting thrust force, Extra Trees aggregates predictions from individual trees. The average of the outputs from M trees is the final forecast y, given an input x. Equation (1) gives the formula for the Extra Tree Regressor. Fig. 3 illustrates the architecture of the model.

$$\hat{y} = \frac{1}{T}\sum_{t=1}^{T} f_t(x)y \tag{1}$$

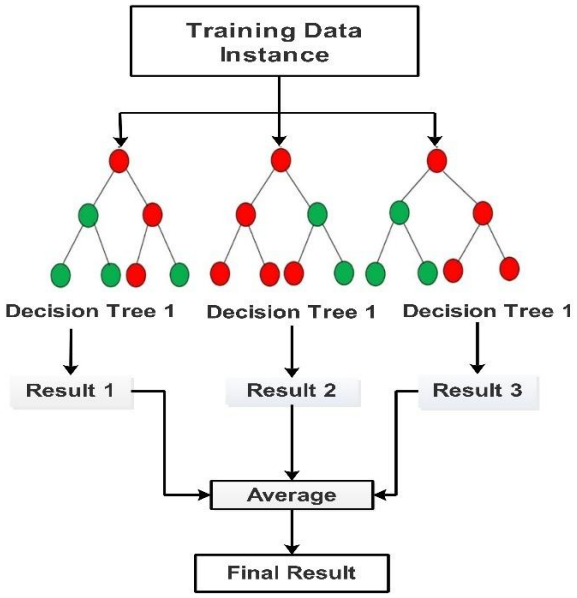


Fig. 3. Architecture of an extra tree regressor

where $f_t(x)$ is the prediction from the t-th tree. During tree construction, for each node, K features are randomly selected (where K is typically the square root of the total features). Split points are chosen uniformly at random from the feature's range, rather than seeking the optimal sciencedirect.com. This method has been applied in various fields, such as stock price forecasting and permeability prediction, demonstrating its efficacy in handling complex, non-linear relationships.

2.3.3 Bagging with Decision Trees

By reducing variance through averaging, Bagging, also known as Bootstrap Aggregating, is a fundamental ensemble approach that Breiman introduced in 1996 to enhance the accuracy and stability of unstable base learners, such as decision trees. In this work, Bagging is applied with Decision Tree Regressors as the base estimators (Bagging (DT)), where bootstrapped subsets of the training data (random samples with replacement) are used to train multiple trees. This method is particularly effective for regression problems like thrust force prediction, as it smooths out the high variance typical of individual decision trees.

The core formula for the bagged prediction $f(x)$ is the average across B bootstrap models, as shown in Equation (2). Fig. 4 illustrates the architecture of the model.

$$\hat{f}(x)=\frac{1}{B}\sum_{b=1}^{n}\hat{f}^{*b}(x) \tag{2}$$

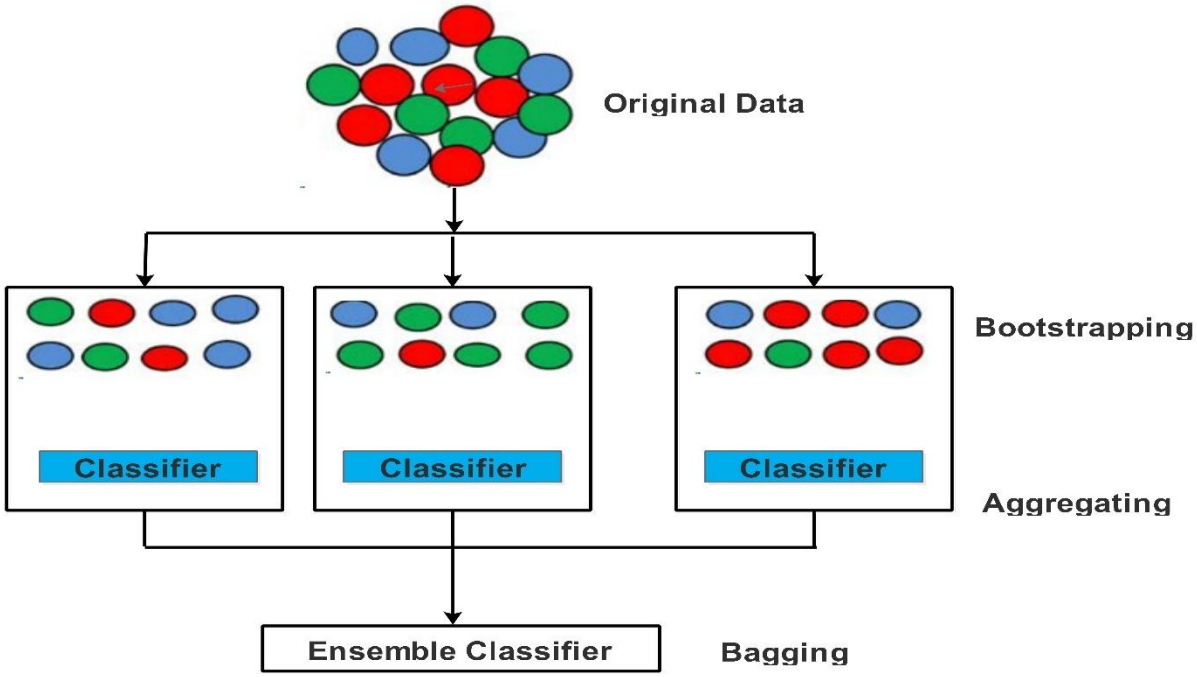


Fig. 4. Architecture of bagging with decision trees

2.3.4 Random Forest Regressor

To further decorrelate the trees and improve model robustness, the popular ensemble approach, Random Forest Regressor, expands on Bagging by adding random feature selection at each node split. To prevent prominent features from dominating the model, it generates numerous decision trees on bootstrapped subsets of the data, but only a random subset of features (usually $\sqrt{p}$ for regression, where p is the total number of features) is considered at each split. Because Random Forest is so good at capturing non-linear correlations and generating feature importance metrics, it is especially well-suited for regression issues like forecasting Thrust Force**.** Fig. 5 illustrates the architecture of the model.

The prediction formula mirrors that of Bagging, but with the added randomness in feature selection, is shown in Equation (3)

$$\hat{y}(x)=\frac{1}{T}\sum_{t=1}^{T}h_t(x) \tag{3}$$

where $h_t(x)$is the result of the t-th tree, which was trained using random feature subsets at splits on a bootstrapped sample. The split criterion often minimizes MSE, defined as in Equation (4)

$$MSE = \frac{1}{n}\sum_{i=1}^{n}(y_i - \hat{y}_i)^2 \quad (4)$$

for n samples in a node.

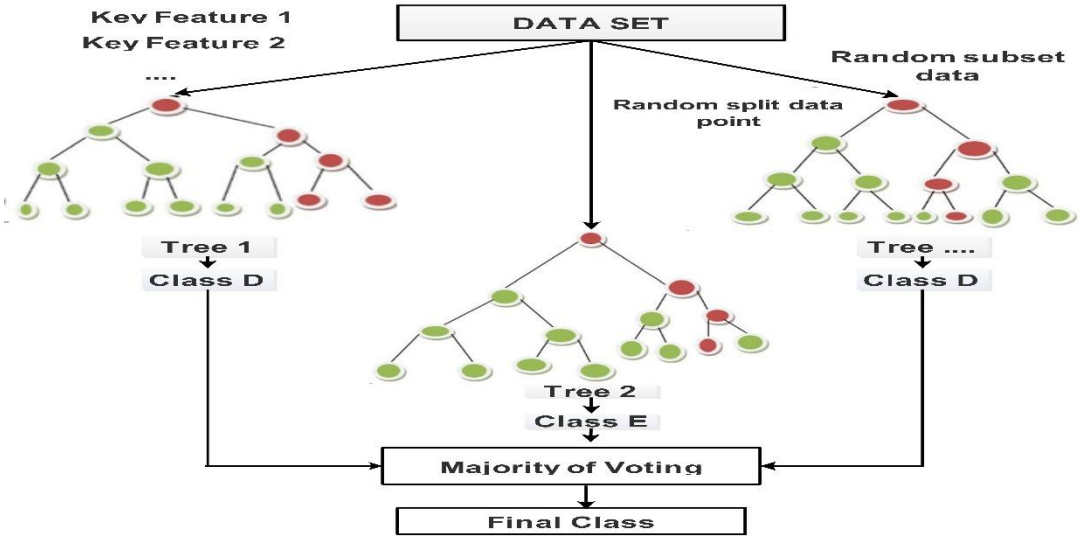


Fig. 5. Architecture of a random forest regressor

2.3.4 Performance evaluation criteria

The dataset generated during the drilling operation was partitioned into 30% for testing and 70% for training to ensure balanced model training and evaluation. The training dataset is prepared using ML techniques, and unused testing data were used to evaluate the performance of the developed model. The following performance evaluation metrics help to identify the most suitable machine learning model to ensure optimal performance and accurate prediction. The formulas for mean absolute percentage error (MAPE), mean absolute difference (MAD), root mean square error (RMSE), standard error (SE), mean square error (MSE), and coefficient of determination (R2) used in performance evaluation are given in equations (5-10).

$$\text{MAPE} = \frac{1}{n}\sum_{i=1}^{n}\frac{\left|F_{e,i} - F_{p,i}\right|}{F_{e,i}} x100 \quad (5)$$

$$\text{MSE} = \frac{1}{n}\sum_{i=1}^{n}(F_{e,i} - F_{p,i})^2 \quad (6)$$

$$\text{RMSE}=\sqrt{\frac{1}{n}\sum_{i=1}^{n}(F_{e,i}-F_{p,i})^2} \tag{7}$$

$$\text{MAD}=\frac{1}{n}\sum_{i=1}^{n}\left|F_{e,i}-F_{p,i}\right| \tag{8}$$

$$\text{SE}=\sqrt{\frac{\sum_{i=1}^{n}(F_{e,i}-F_{p,i})^2}{n-2}} \tag{9}$$

$$R^2=1-\frac{\sum_{i=1}^{n}(F_{e,i}-F_{p,i})^2}{\sum_{i=1}^{n}(F_{e,i}-\overline{F}_{e,i})^2} \tag{10}$$

Where n indicates the quantity of samples, $F_{e,i}$ indicate the actual value $F_{p,i}$ indicates the predicted value and $\overline{F}_{e,i}$ indicates the mean of the actual value

3 Results and discussion

The aim is to predict F_z and F_t using ML models such as Extra Trees, Bagging, and Random Forest. This study aims to achieve high-quality drilling of a WPC composite panel using a coated carbon steel tool with an aluminum finish. The input parameters chosen for the drilling process, SS, FR, and DD, were fed to the model for predicting the F_z and F_t. Various machine learning models were utilized. The RSM model is often created utilizing a number of process factors to predict the output responses. The data were generated from various signals during the experiment. However, data received from various signal sources during the experiment requires significant time to become an expert. The RSM model's findings cannot be applied to other process materials. Nevertheless, by providing the input values, the suggested approach seeks to predict the F_z and F_t. Three input parameters were used to build the dataset, which was then modeled using machine learning methods to predict the F_z and F_t. The CNC drilling machine used the three input parameters to predict F_z and F_t. Because the input features and output responses were quantitative in nature, RSM models were employed.

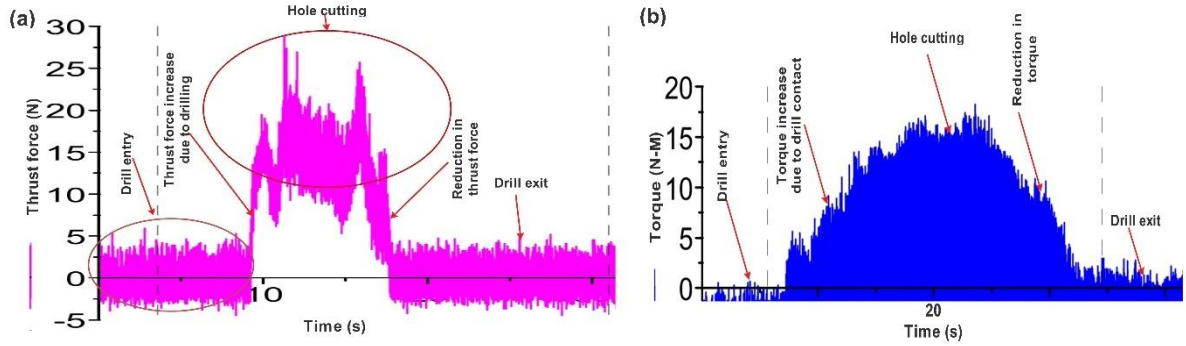


Fig. 6. Response graph of a) F_z, b) F_t, for various drilling parameters.

The F_z and F_t are essential elements in drilling wood composite material because they influence drilling efficiency, tool performance, and hole quality of the machined surface. F_z is defined as an axial force acting along the feed direction of the tool during machining, resulting from the resistance of the material against the tool's penetration. Meanwhile, F_t is defined as the rotational force acting on the drill around its axis during material removal. This causes shear deformation during drilling by the drill lips, as the resistance to rotation is caused by the material. A Kistler multicomponent dynamometer, type 9257 B, installed beneath the workpiece fixture, is used to measure the F_z and F_t produced during the drilling of the WPC composite panel. A charge amplifier (Model 5070B) is attached to the dynamometer to transform the piezoelectric signal into an equivalent electric voltage. Dynamometer software is used to process the gathered data, which is then summarized in Table 3. Fig. 6 illustrates the graphs obtained from the Kistler dynamometer for the output response (F_z and F_t) of experiment no.10.The F_z and F_t values obtained during the measurement correspond to the peak (maximum) values obtained from the cutting force measurement during each drilling operation

Table 3 Experimental design and results

Run Number	Inputs			F_z-(N)			F_t-(N-m)		
	N **(rpm)**	***f*** **(mm/min)**	***d*** **(mm)**	**Run -1**	**Run -2**	**Run-3**	**Run-1**	**Run-2**	**Run-3**
1	1000	75	6	12.59	12.09	11.59	13.83	14.33	14.83
2	1000	75	8	10.98	12	12.24	13.62	14	14.74
3	1000	75	10	14.13	14.63	15.13	17.29	17.79	18.29
4	1000	150	6	13.12	13.5	13.4	14.45	15.23	15.68
5	1000	150	8	14.93	15.43	15.93	15.95	16.45	16.95
6	1000	150	10	15.89	16	16.47	18.3	18.8	19.54
7	1000	225	6	17.16	17.66	18.16	18.88	19.38	19.88
8	1000	225	8	16.75	17	17.61	19.12	19.89	20.85
9	1000	225	10	19.59	20.09	20.59	20.73	21.23	21.73
10	2000	75	6	10.89	11.4	11.4	10.35	10.8	12.09
11	2000	75	8	12.21	12.71	13.21	12.03	12.53	13.03
12	2000	75	10	13	13.4	13.38	14.25	14.4	15.15
13	2000	150	6	12.54	13.04	13.54	13.81	14.31	14.81
14	2000	150	8	13.55	13.8	14.59	14.4	14.8	15.71
15	2000	150	10	17.64	18.14	18.64	17.13	17.63	18.13
16	2000	225	6	14	14.5	15.69	16.8	17	17.56
17	2000	225	8	17.48	17.98	18.48	18.35	18.85	19.35
18	2000	225	10	17.12	18	18.55	20.8	21.2	21.69
19	3000	75	6	10.42	10.92	11.42	10.72	11.22	11.72
20	3000	75	8	10.12	11	10.86	10.95	12	12.6
21	3000	75	10	13.27	13.77	14.27	12.28	12.78	13.28
22	3000	150	6	11.12	11.56	12.96	12.6	13	13.73
23	3000	150	8	14.24	14.74	15.24	14.23	14.73	15.23
24	3000	150	10	13.85	14.7	15.43	16.2	16.7	16.9
25	3000	225	6	14.66	15.16	15.66	15.63	16.13	16.63
26	3000	225	8	14.12	14.5	14.55	16.95	17.95	18.65
27	3000	225	10	19.48	19.98	20.48	19.51	20.01	20.51

3.1 Experimental values

Table 3 shows the output responses obtained from the multicomponent Kistler Dynoware using Taguchi's L27 orthogonal array. The experiment is performed three times to improve the reliability and accuracy of the measuring system and reduce random experimental error. Table 3 shows that as SS increases from 1000 to 3000 rpm, F_z and F_t decrease. This indicates that higher SS leads to increased frictional heating. The heating softens the polymer matrix, reducing cutting resistance and thus F_z and F_t. Both F_z and F_t increase with DD, from 6 to 10mm. A larger diameter engages more material and increases contact area and radius, which increases F_z and F_t. Additionally, F_z and F_t decrease with a lower FR. For example, at 3000 rpm and 10mm diameter, F_z and F_t drop from 20.48 N and 20.21 N · m at 225 mm/min to 14.27 N and 13.38 N · m at 75 mm/min. At lower FR, the material removal rate per revolution decreases, resulting in minimum F_z and F_t, which matches previous literature results[68]. From the table, it can be concluded that 3000 rpm, 75 mm/min, and 6 mm result in the minimum F_z and F_t

To determine the extent of subsurface flaws and the impact of drilling parameters on hole quality and structural integrity of the WPC composite, a more thorough examination of damage within the drilled hole was conducted. Figure 7 presents SEM micrographs of the interior of the drilled hole. The images, captured at magnifications of 206X and 1.2KX, reveal that the wood fibers are well bonded with the thermoplastic matrix, such as polyethylene and polypropylene. These micrographs correspond to a drilled surface produced under conditions of 2000 rpm, 150 mm/min, and 8 mm, with an average F_z of 13.55N and F_t of 14.4 N · m. Under these conditions, the composite panel exhibits significant surface cavities, micro-cracks, fiber fracture, surface irregularity, and filler particles. These defects are likely caused by thermal softening of the material during drilling at intermediate SS, FR, and DD.

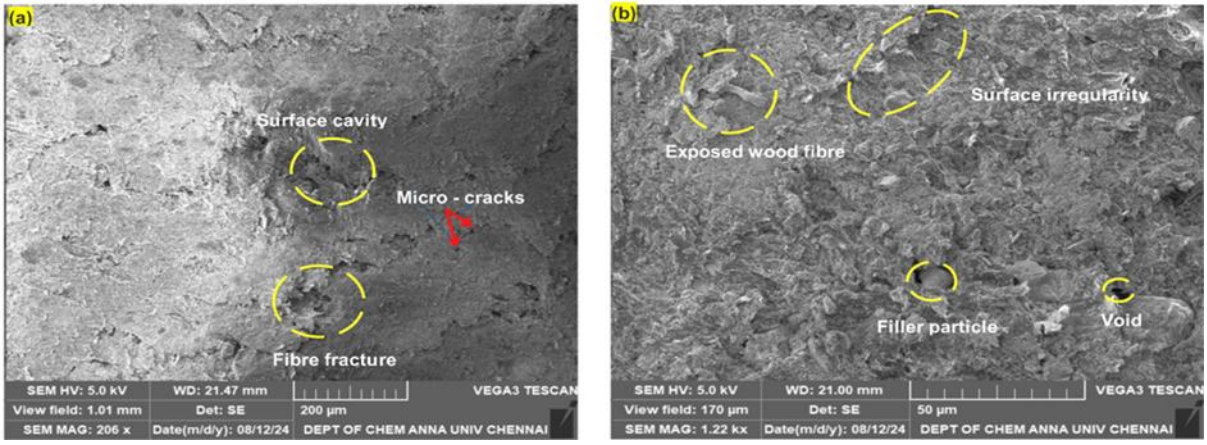


Fig. 7. SEM images observed during the drilling of the WPC composite. (Experiment No.14, Trial 1)

3.2. Correlation between input parameters and output responses

3.2.1. Heat maps

An overview of the relationship between the drilling parameters and output responses is given by the Pearson correlation coefficient. Fig. 8 shows a heat map of the Pearson correlation between the output response (F_z and F_t) and the input parameters (N, f, and d). The pairwise correlation coefficient is calculated between the input and output responses. The range of the correlation is -1 to +1. A strong positive association is indicated by values closer to 1; a strong negative association is indicated by values closer to -1; and a non-significant linear correlation is indicated by values near 0. According to the figure analysis, there is a significant positive association between F_t and FR, as well as F_z and FR. This implies that whereas a decrease in FR results in a fall in both Fz and Ft, an increase in FR causes both F_z and F_t to increase. The moderate positive correlation among F_z, F_t, and DD indicates that DD plays a significant role in influencing F_z and F_t. On the other hand, negative correlations are observed among F_z, F_t, and SS, indicating that an increase in SS tends to lower F_z and F_t and improve the surface quality of the drilled hole.

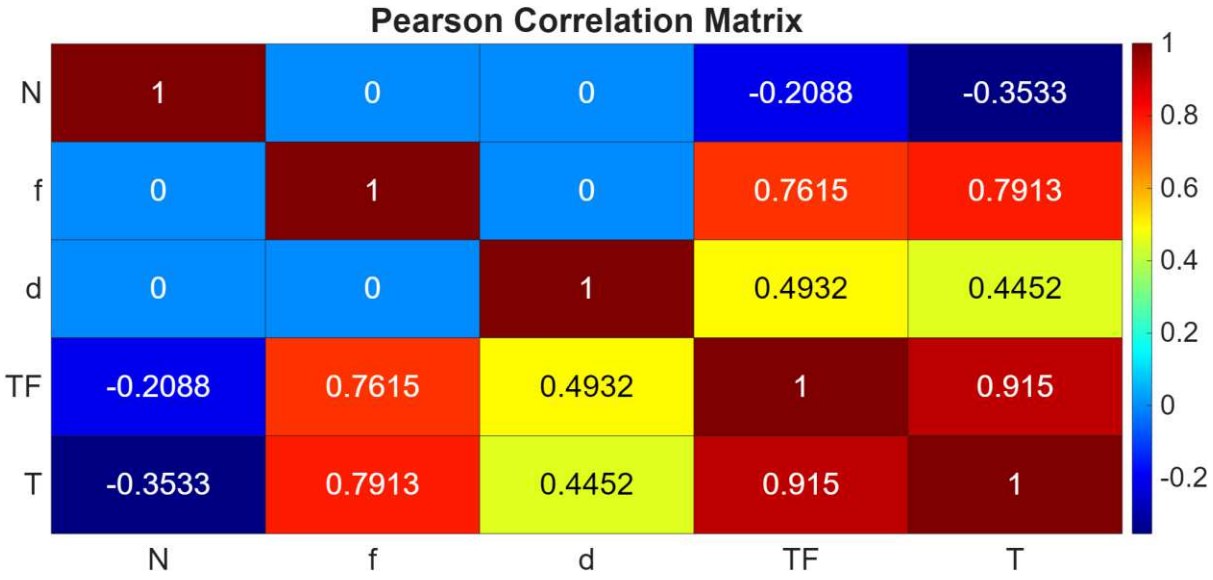


Fig. 8. Pearson correlation between process parameter and output responses.

ANOVA is a statistical tool used to assess how various process parameters affect the output responses F_z and F_t. Additionally, it establishes the conditions and optimal process parameters, and it can identify the key elements necessary for process enhancements. ANOVA is employed in this study to assess the impact of parameters on F_z and F_t and to identify the key elements needed to develop ML models. This study uses ANOVA at the 95% confidence level with a p-value less than 0.05. Table 4 displays the ANOVA results for F_z and F_t. The ANOVA results show $p<0.05$, indicating that the developed model is significant at the 95% confidence level. The F-value of the F_z model is 50.83, with an R^2 of 86.56% and a predicted R^2 of 82.70%. The generated model predicts F_t with $p<0.05$(F_t: F-value=143.20, R^2 =94.78% and anticipated R^2 =93.03%). In Table 4, the most significant factor is the FR, followed by DD and SS.

Table 4 Analysis of F_z and F_t using ANOVA in drilling WPC

Source	**Sum of squares**		**df**	**Mean square**		**F-value**		**p-value**		**P (%)**		**Remarks**
	F_z	**F_t**		**F_z**	**F_t**	**F_z**	**F_t**	**F_z**	**F_t**	**F_z**	**F_t**	
Model	494.93	685.06	9	54.99	76.12	50.83	143.20	0.0001	< 0.0001	-	-	significant
N	24.24	87.96	1	24.24	87.96	22.41	165.48	< 0.0001	< 0.0001	4.90	12.84	
f	322.52	441.24	1	322.52	441.24	298.10	830.10	< 0.0001	< 0.0001	65.16	64.41	
d	135.28	139.68	1	135.28	139.68	125.04	262.79	< 0.0001	< 0.0001	27.33	20.39	
Nf	1.24	3.64	1	1.24	3.64	1.15	6.85	0.2874	0.0108	0.25	0.53	
Nd	1.82	0.0049	1	1.82	0.0049	1.68	0.0092	0.1985	0.9238	0.37	0.00	
fd	2.24	0.4225	1	2.24	0.4225	2.07	0.7948	0.1550	0.3757	0.45	0.06	
N^2	0.1318	2.64	1	0.1318	2.64	0.1218	4.97	0.7281	0.0290	0.03	0.39	
f^2	0.6235	3.97	1	0.6235	3.97	0.5763	7.47	0.4503	0.0079	0.13	0.58	
d^2	6.83	5.49	1	6.83	5.49	6.32	10.33	0.0142	0.0020	1.38	0.80	
Residual	76.82	37.74	71	1.08	0.5315	-	-	-	-	15.52	5.51	
Lack of Fit	61.19	19.56	17	3.60	1.15	12.44	3.42	< 0.0001	0.0003	12.36	2.86	significant
Pure Error	15.62	18.18	54	0.2893	0.3367	-	-	-	-	3.16	2.65	
Cor Total	571.75	722.80	80									
Std. Dev.	1.04	0.7291										
R^2	0.8656	0.9478										
Adjusted R^2	0.8486	0.9412										
Predicted R^2	0.8270	0.9302										
PRESS	98.90	50.46										

3.2.2 Main effects plot for SS, FR, and DD

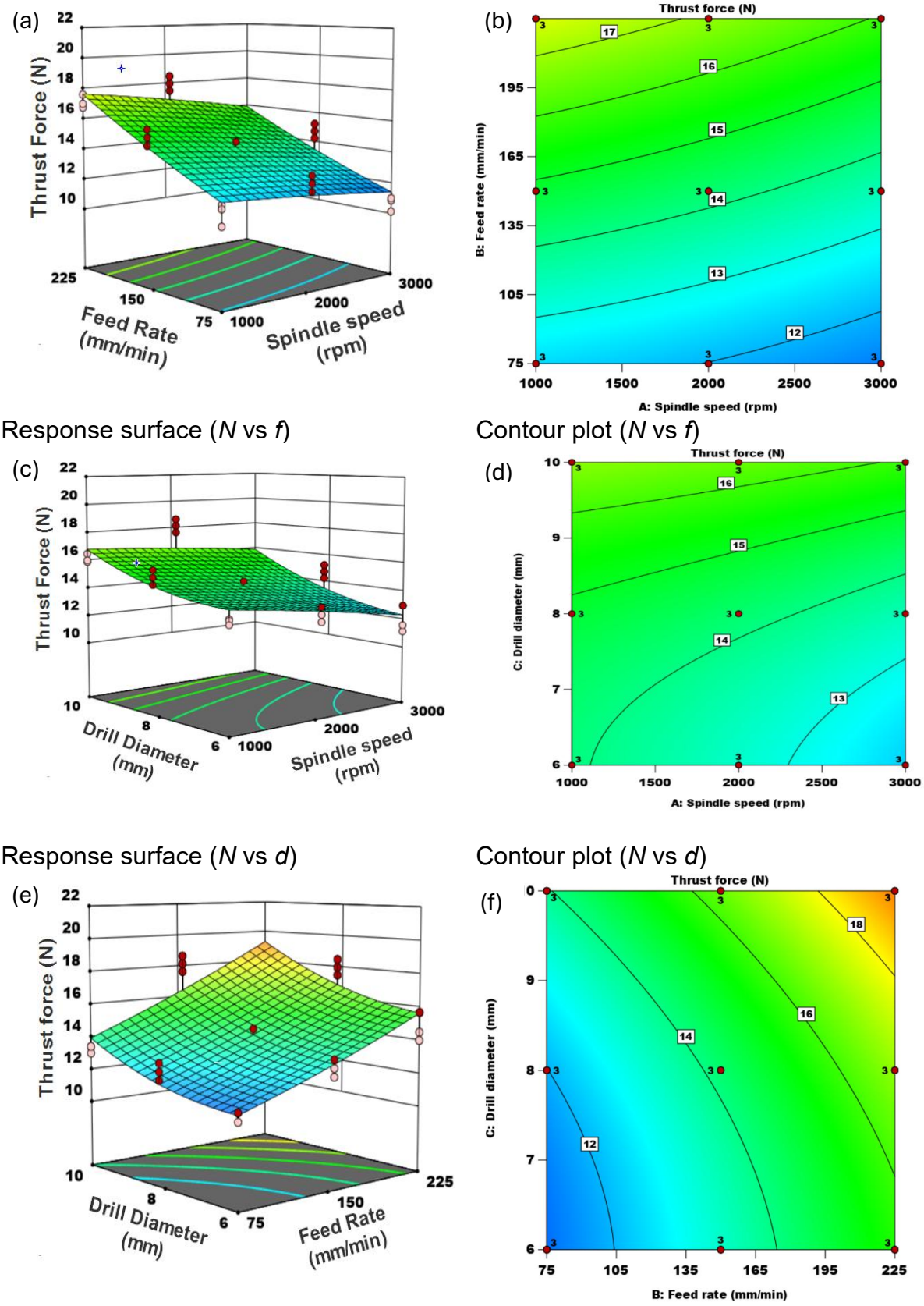
3.2.2.1 Analysis of thrust force (F_z)

The effect of SS and FR on F_z is shown in Fig. 9(a). The response contour plot based on this data is presented in Fig. 9(b). As seen in Fig. 9(b), the lowest F_z of 12N occurs when using a high SS of 3000 rpm combined with a low FR of 75 mm/min. This is because higher SS and lower FR reduce the chip load per revolution and improve cutting efficiency, lowering resistance to tool penetration in the WPC composite and resulting in a minimum F_z. In contrast, the contour suggests that a low SS of 1000 rev/min and a high FR of 225 mm/min yield a high F_z of 17N. This is due to a large uncut chip thickness and less efficient cutting action, which increases resistance to material removal and results in higher Fz. Fig. 9(c) displays the influence of SS and DD on F_z. Its response surface is shown in Fig. 9(d). From this figure, the minimum F_z of 13N occurs at a high SS of 3000 rpm and a small DD. At higher SS, the cutting edges remove material more effectively due to enhanced shearing action and reduced frictional resistance. Simultaneously, a smaller DD decreases the cross-sectional area of material being removed and reduces the contact length between the drill and the workpiece. These factors collectively lower resistance to tool penetration, resulting in reduced F_z. The minimum F_z occurs at a medium SS of 2000 rpm and a smaller DD, which yields a higher Fz of 16N. The cutting efficiency is not high enough to compensate for the concentrated cutting load at a smaller DD, resulting in increased resistance to penetration and higher F_z. In contrast, a medium SS of 2000 rpm, combined with a larger DD, results in a higher F_z of 16N. A larger DD increases the contact area and material removal resistance, and at medium SS, the cutting efficiency is not high enough to offset this increased load, leading to a higher F_z. Fig. 9(e) illustrates the impact of FR and DD on F_z, while Fig. 9(f) shows their response surface. From Fig. 9(f), it is observed that the lowest F_z of 12N occurs with a low FR of 75 mm/min and a DD of 6mm. A low FR reduces chip thickness, and a smaller DD reduces the contact area; together, these factors decrease resistance to tool penetration and produce a minimum F_z. Conversely, a higher FR of 225 mm/min and a DD of 10mm produce an F_z of 18N. This is due to increased cutting load and chip formation resistance during drilling. Thus, from the above discussion, it has been found that F_z is minimum at a maximum SS of 3000 rpm, FR of 75mm/min, and DD of 6mm. A high FR increases chip thickness, and a larger DD increases the contact area and material

removal load; together, these factors significantly increase resistance to penetration, resulting in higher F_z.

3.2.2.2 Analysis of torque (F_t)

Fig. 10(a) illustrates how SS and FR influence Ft, with the response contour in Fig. 10(b). The lowest F_t of 12 N-m occurs at a high SS of 3000 rpm and a low FR of 75 mm/min. High SS boost cutting efficiency, and lower FR reduces the material removal load per revolution; together, these decrease the rotational resistance on the drill, lowering Ft. Conversely, a lower SS of 1000 rpm with a higher FR of 225 mm/min results in a higher F_t of 18 N-m. At higher FR, the drill removes more material per turn, increasing shear resistance and friction. Lower SS slow cutting, making shearing less efficient and increasing contact time with the workpiece. These factors make drilling more difficult with WPC, raising F_t. Fig. 10(c) shows how SS and DD affect F_t, with the response surface in Fig. 10(d). A minimum F_t of 14 N-m occurs at 3000 rpm and a small DD of 6 mm. Higher SS increases cutting velocity, enhancing the shearing of fibers and thermoplastic matrix. A smaller DD reduces the cutting-edge length and the radial distance from the center, decreasing the moment needed to rotate the drill. These combined effects lower friction and shear resistance, reducing F_t during drilling. Conversely, a medium SS of 2000 rpm and a larger DD of 10 mm result in a higher F_t of 18 N-m. Larger DD requires more rotational force due to increased moment arm and friction. At medium SS, the cutting velocity is moderate and may not sufficiently reduce resistance, leading to higher F_t. Fig. 10(e) shows the effects of FR and DD on F_t, with the response surface in Fig. 10(f). The lowest F_t of 12 N-m occurs at a low FR of 75 mm/min and a DD of 6 mm, as a lower FR minimizes material removal per revolution, reducing shear resistance. A smaller DD also decreases the cutting-edge length and radial distance, thereby reducing the F_t required to rotate the drill. These factors collectively lower friction and shear resistance, decreasing torque. Conversely, an FR of 225 mm/min and a 10 mm DD result in a torque of 20 N-m. Higher FR removes more material per turn, increasing shear resistance. A larger DD also increases the cutting-edge length and radial distance, raising the moment needed for rotation, which increases frictional and shear resistance and F_t. In summary, the minimum F_t occurs at a maximum SS of 3000 rpm, FR of 75 mm/min, and DD of 6 mm. When drilling particleboard composites, a similar pattern was noted, with FR having the greatest impact on cutting force[66]. These results confirm that FR is the primary parameter affecting cutting force in WPC panels.

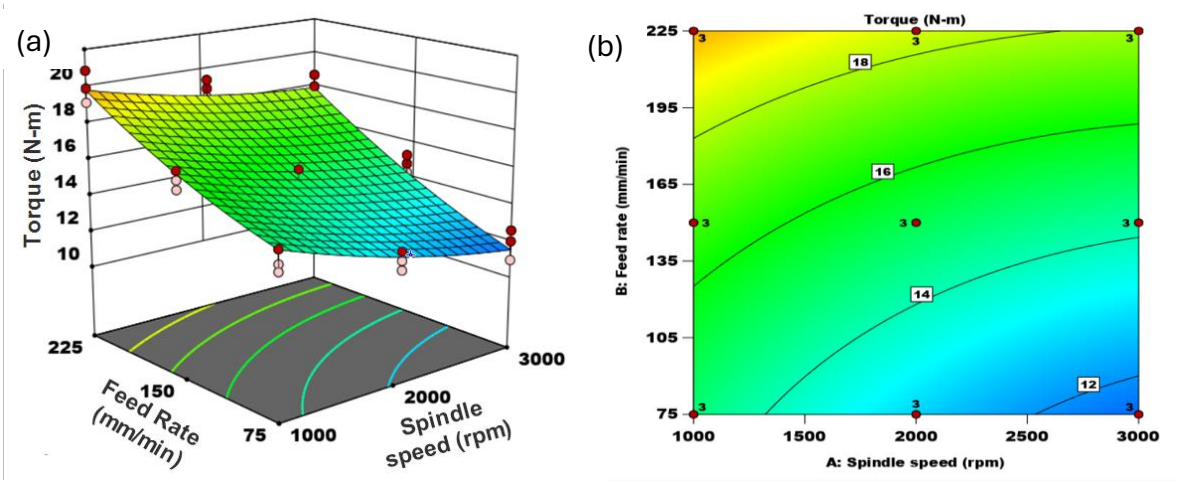


Response surface (*N* vs *f*) Contour plot (*N* vs *f*)

Response surface (*N* vs *d*) Contour plot (*N* vs *d*)

Response surface (*f* vs *d*) Contour plot (*f* vs *d*)

Fig. 9. Response surface of thrust force and its contour plot



Response surface (*N* vs *f*) Contour plot (*N* vs *f*)

Response surface (*N* vs *d*) Contour plot (*N* vs *d*)

Response surface (*f* vs *d*) Contour plot (*f* vs *d*)

Fig. 10. Response surface of torque and its contour plot

4 Application of ML models for the prediction.

In this study, three single ML models, namely Extra Trees, Bagging trees with decision trees, and Random Forest, were selected for modeling and prediction. The machine learning models were chosen for their short computation time and high predictive accuracy. Fig. 11 shows the proposed scheme for predicting response using a machine learning technique. To monitor overfitting and underfitting in the developed model before predicting the output response, epoch-wise trends were generated to track model performance and identify overfitting. In this prediction of F_z and F_t, an epoch-wise trend was used before predicting F_z and F_t with the three ML models. To assess the developed models' performance, six performance evaluation metrics, such as MAD, MSE, RMSE, MAPE, SE, and $R^{2,}$ were used to compare the outcomes from the established models.

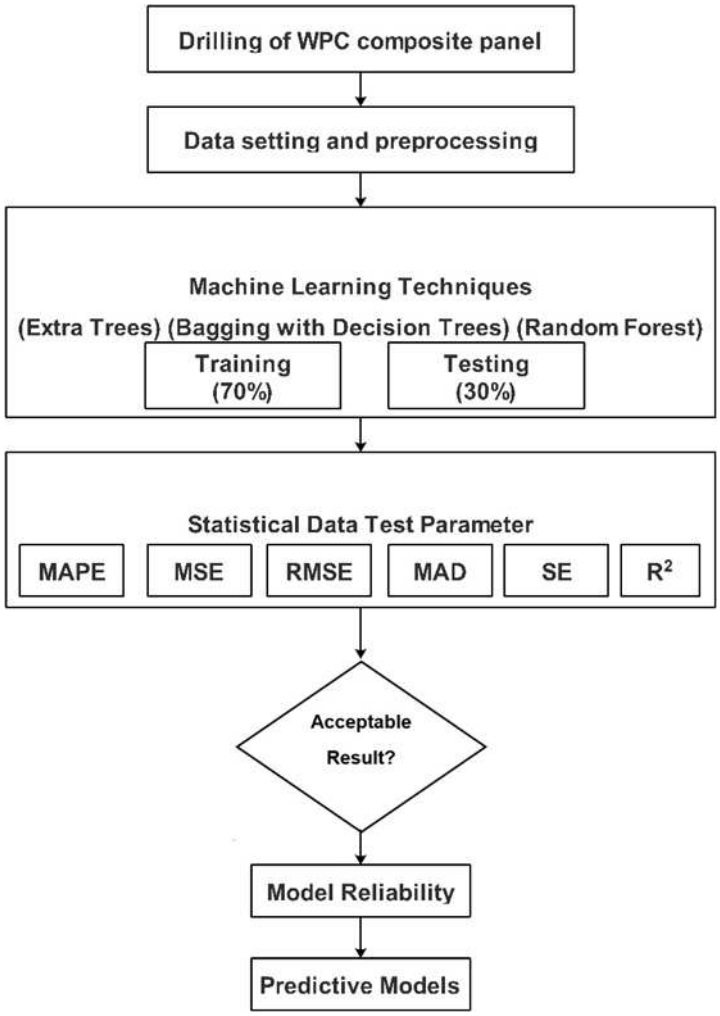


Fig.11. Proposed scheme for predicting response parameter.

4.1 Epoch-Wise RMSE Trends F_z:

The RMSE plot for thrust force, shown in Fig. 12, demonstrates that Extra Trees remains at a nearly constant error of 0.673 across all epochs, indicating rapid stabilization and little to no benefit from additional estimators beyond the initial estimate. Bagging (DT) and Random Forest show steeper declines early on, beginning from outliers starting at higher errors, epochs 1-3 for Bagging: (0.758, 0.866, 0.739) and then levelling off to lower errors around epochs 14-15 with lower errors of 0.53-0.51 or a marginal decrease from there. XGBoost early epochs also show extreme sensitivity, with outliers at epochs 1 through 4 (1: 2.241, 2: 1.784, 3: 1.460, 4: 1.233), but were not the focus of this study. The good news is that Bagging and Random Forest use the extra estimates to further reduce variance in F_z prediction, which is an important variable during drilling to mitigate delamination in composite materials. Extra Trees remained at a more stable RMSE throughout the iteration periods on thrust force measurements around 0.675, indicative of stabilization compared to the other models, likely from extreme randomization. The Bagging (DT) model showed a rapid decline from their first epoch (epoch 1: 0.758) to around 0.527 by epoch 15, with marginal decline thereafter. Random Forest followed a similar trend, stabilizing at 0.514. XGBoost exhibited significant outliers (epochs 1: 2.241, 2: 1.784), indicating slower convergence, with values like 1.233 at epoch 4 still high compared to ensembles.

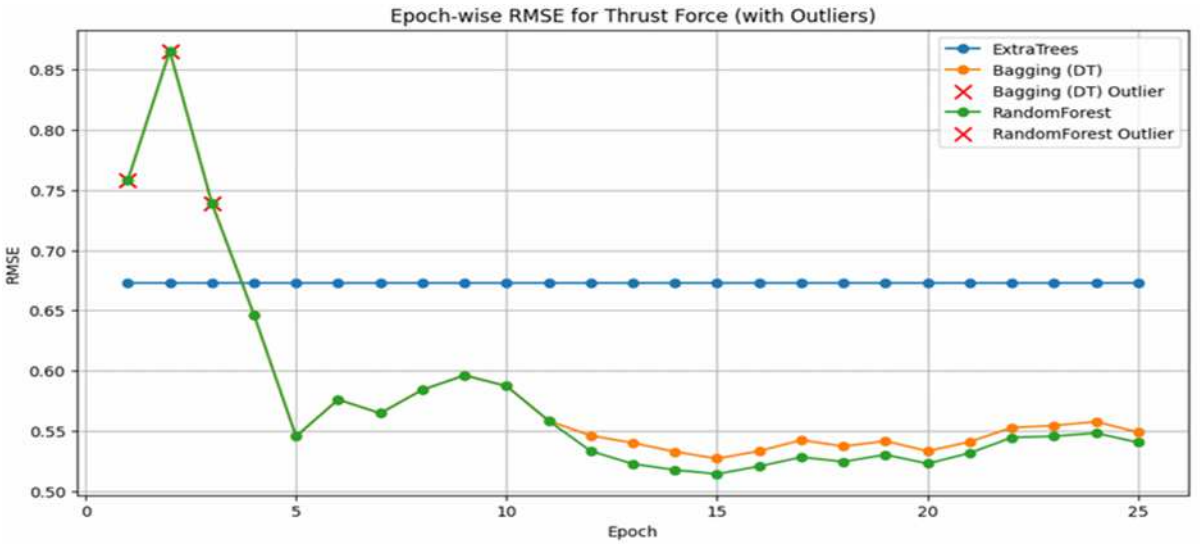


Fig. 12. Epoch-wise RMSE analysis for thrust force

4.2 Epoch-Wise RMSE Trends of Torque:

Fig. 13 shows epoch-wise RMSE analysis of F_t, where similar patterns emerge, with Extra Trees constant at approximately 0.732. Bagging (DT) and Random Forest decrease from initial outliers (Bagging epochs 1-3: 0.816, 0.973, 0.851) to stabilized

values near 0.56-0.55 by epoch 25. XGBoost shows more pronounced early outliers (epochs 1-6: 2.325, 1.804, 1.427, 1.174, 0.987, 0.856), underscoring the need for sufficient boosting rounds. The convergence indicates improved F_t prediction with more trees, essential for energy efficiency and tool life in high-speed drilling. Extra Trees remained stable at 0.732, while Bagging (DT) dropped from an outlier (epoch 1: 0.816) to 0.557. Random Forest converged to 0.549, showing resilience. XGBoost outliers (epochs 1: 2.325, 2: 1.804) diminished to 0.856 by epoch 6, suggesting a need for more iterations to match ensemble performance.

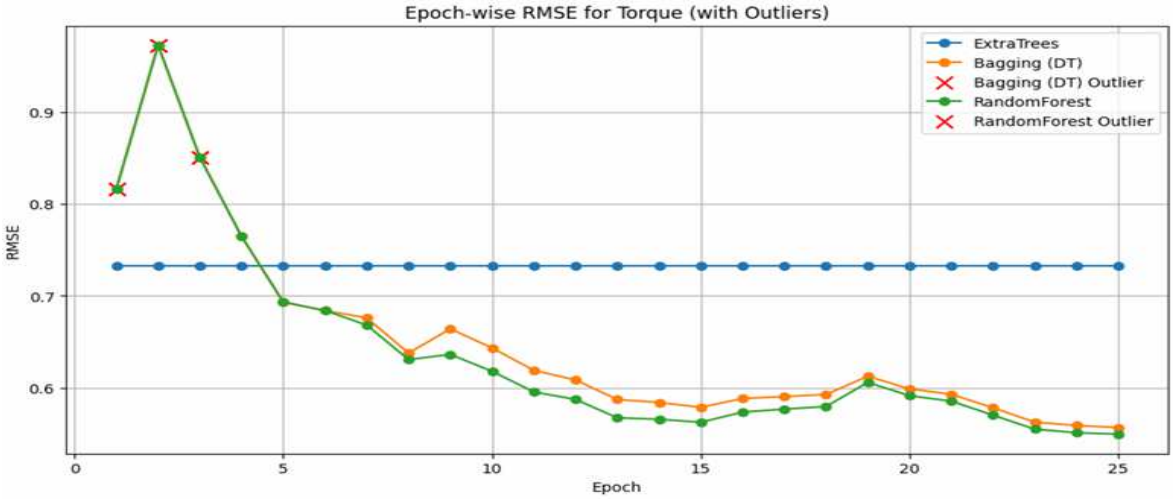


Fig. 13. Epoch-wise RMSE analysis for torque

4.3 Comparing experimental and predicted values of F_z and F_t

Three machine learning models (Bagging decision trees, Random Forest, and Extra Trees) were used to predict the output responses (F_z and F_t) in a WPC drilling operation. The models were trained and tested on 81 data points from the experimental dataset to predict the output responses. 30% of the dataset was used for testing and model evaluation, and the remaining 70% was used for training. Figures. 14 and 15 show the comparison between actual and predicted values for F_z and F_t, corresponding to variations in SS, FR, and DD across the 27 experimental runs of the three-trial experiment, using bagging decision trees, random forests, and extra trees. The diagram clearly provides valuable insights into the accuracy of the three models between actual and predicted values. Six performance indicators, defined by equations 5-10, were used as quantitative measures of model performance. Tables 5 and 6 present the comparative analysis of all three models. This performance analysis helps researchers ensure accurate and reliable predictions of F_z and F_t.

The analysis of the results in Tables 5 and 6 indicates that the random forest model performs better than the other two models. Specifically, for F_z, the random forest model achieved a MAPE of 1.6021, MSE of 0.075, RMSE of 0.275, MAD of 0.231, SE of 0.280, and R^2 of 0.998, whereas for F_t it achieved a MAPE of 0.718, MSE of 0.0197, RMSE of 0.1406, MAD of 0.1083, SE of 0.143, and R^2 of 0.997. All three models performed well, with R^2 greater than 0.988. The random forest model outperformed the bagging model, and the bagging model outperformed extra trees. In conclusion, all three models performed well in predicting F_z and F_t from the experimental dataset.

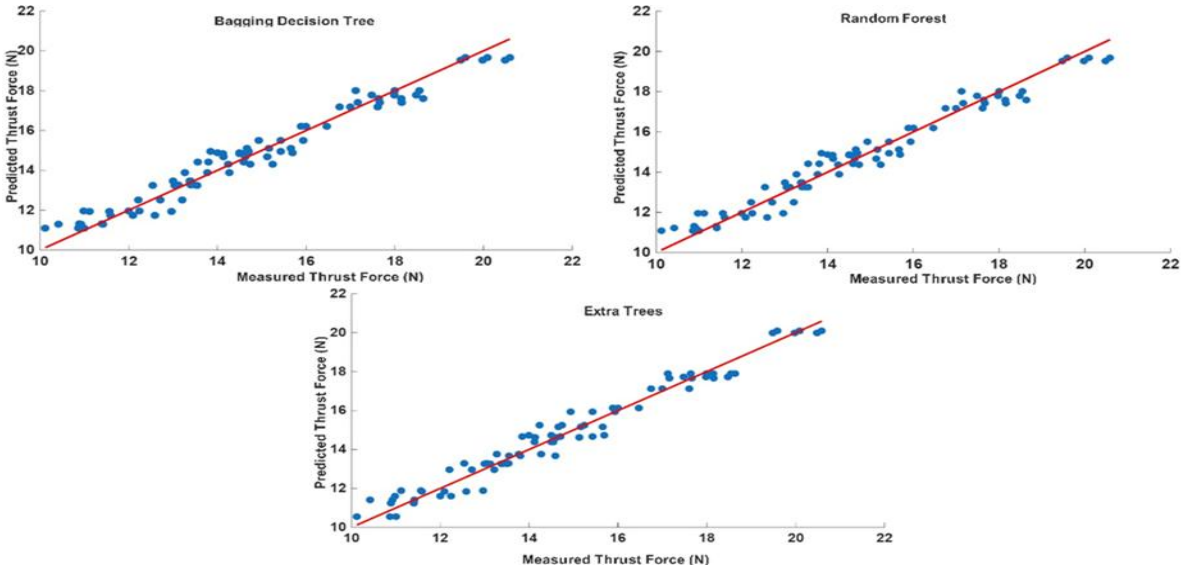


Fig. 14. Comparison of Experimental and predicted F_z using various machine learning algorithms

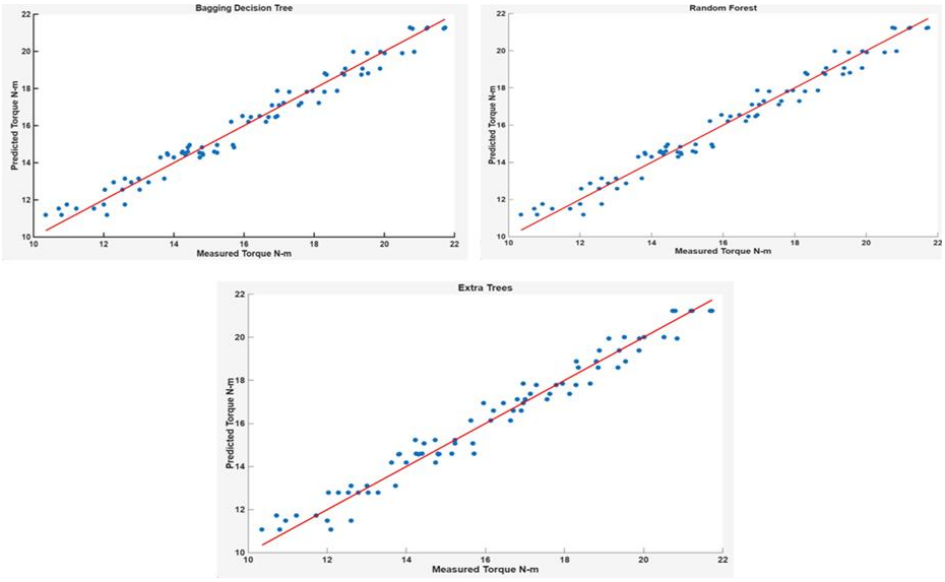


Fig. 15. Comparison of Experimental and predicted F_t using various machine learning algorithms

Table 5

Statistical analysis of three models for the prediction of F_z

Models	MAPE	MSE	RMSE	MAD	SE	R^2
Extra Trees	0.916	0.044	0.209	0.124	0.213	0.993
Bagging	1.645	0.079	0.282	0.236	0.288	0.988
Random Forest	1.601	0.075	0.275	0.231	0.280	0.998

Table 6

Statistical analysis of three models for the prediction of F_t

Models	MAPE	MSE	RMSE	MAD	SE	R^2
Extra Trees	0.9461	0.049	0.223	0.1337	0.227	0.994
Bagging	0.7591	0.0231	0.1522	0.114	0.155	0.997
Random Forest	0.718	0.0197	0.1406	0.1083	0.143	0.997

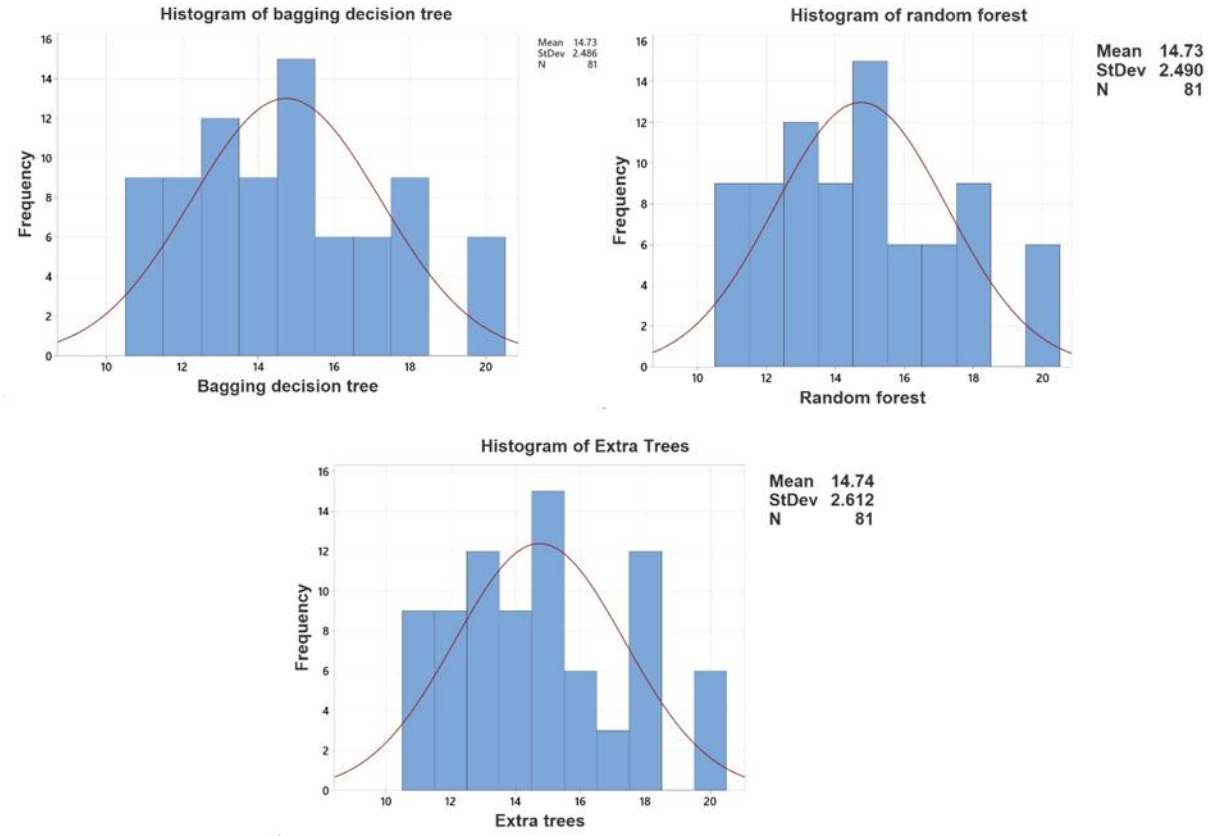


Fig. 16. illustrates the error histogram for F_z prediction using ML models

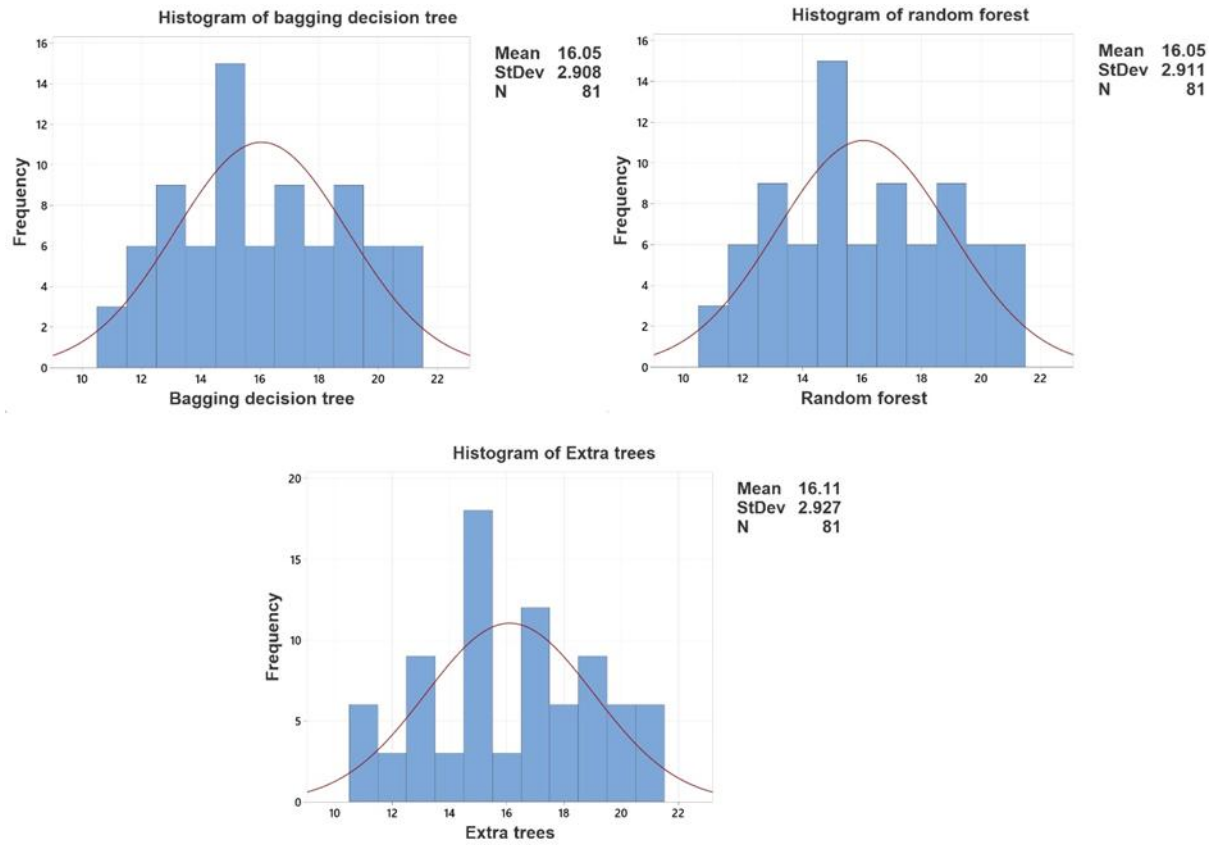


Fig. 17. illustrates the error histogram for F_t prediction using ML models

Figures. 16 and 17 display the histogram of prediction model error of Random forest, Extra tree, and Bagging model in the prediction of F_z and F_t of WPC composite panel. The figure analysis shows that the data are distributed symmetrically with no significant outliers, indicating that the developed model is performing well with a stable prediction of the model with an error distribution around zero. All three models recorded the smallest amount of error with a higher amount accuracy. In conclusion, the random forest outperforms extra trees, and extra trees outperform bagging.

Figures. 18 and 19 show Anderson-Darling normality plots used to check how predicted values are distributed for the decision tree, random forest, and bagging models. In these plots, data points should form a straight line if the distribution is normal. The random forest model comes closest to this, with an Anderson-Darling value of 1.175 and a P-value below 0.005 for F_z, and a value of 0.924 with a P-value of 0.018 for F_t. These results suggest that the random forest model's predictions are more normally distributed, which points to higher accuracy and reliability compared to the other models.

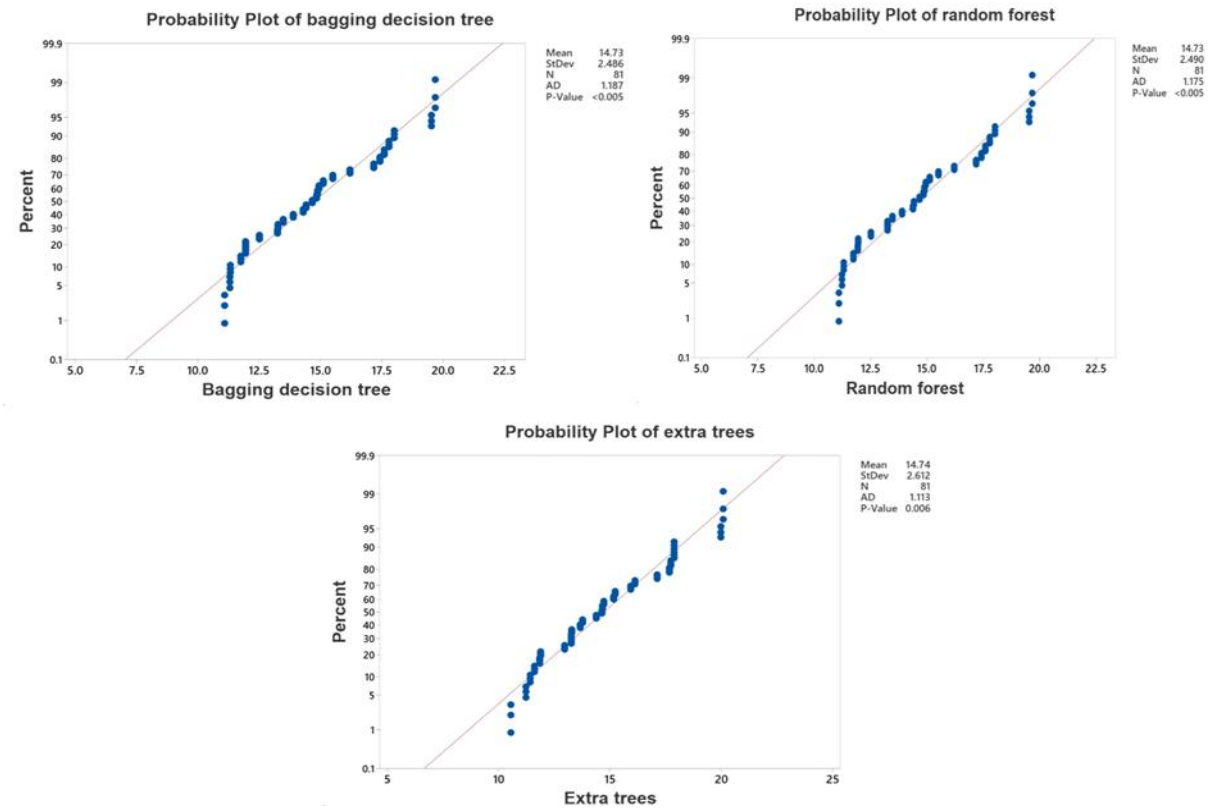


Fig. 18. Anderson-Darling analysis for the prediction of F_z using a machine learning algorithm

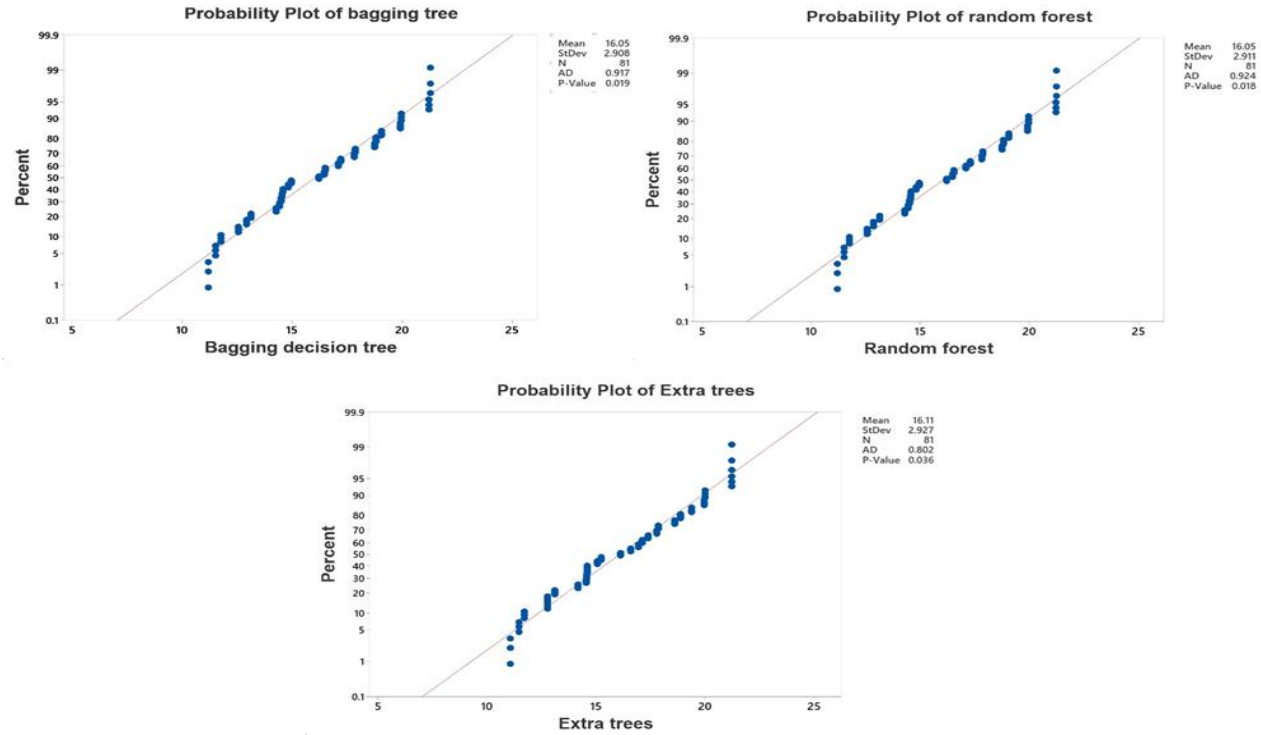


Fig. 19. Anderson-Darling analysis for the prediction of F_t using a machine learning algorithm

5. Conclusion

The study compares the effectiveness of different machine learning models in predicting Fz and Ft, and shows the relationship between machining parameters and the output responses (Fz and Ft) in drilling WPC composite panels using a carbon steel with an aluminum finish and three drill diameters (6, 8, and 10mm).In the present investigation, three SS and three FR were used across the three DD. The key findings can be summarized as follows.

(i)The most significant machining parameters affecting F_z and F_t were determined to be FR, followed by DD and SS. The lowest F_z and F_t, 10.66 N and 11.22 N-m, were obtained at 3000 rpm, 75mm/min, and 6mm. The highest F_z and F_t of 20.09 N and 21.23 N-m were obtained at 1000 rpm,225mm/min, and 10mm.

(ii) The ANOVA analysis of F_z and F_t reveals that the ranking of the best process parameters was statistically significant for the response variable. The ANOVA results reveal that FR contributes the most substantially (65.16%) to F_z, with DD (27.33%) and SS (4.90%) also showing significant impact. On the other hand, F_t is primarily influenced by FR (64.41%), followed by DD (20.39%) and SS (12.84%).

(iii)The drilling operation and machine learning applications have provided valuable insights into the effects of drilling parameters on F_z and F_t.

(iv) Random Forest outperforms bagging and extra trees in the prediction of F_z and F_t, achieving R^2 scores of 0.998 and 0.997.

(v) Strong correlations were validated by experimental and machine learning model predictions, and the suggested model produced respectable outcomes with comparatively high prediction accuracy.

6. Future work

The study focused on estimating Fz and Ft during WPC drilling using a machine learning algorithm and minimal process parameters, with carbon steel and an aluminum finish. The scope of the study can be expanded through the following future work. (i)Estimation of F_z, F_t, F_d, R_a, circularity error, and cylindricity error using different single and hybrid machine learning models. (ii)Drilling operations can be performed using different tool materials, tool geometry, and tool coating. (iii)Drilling operations can be performed using the MQL concept to minimize the temperature, tool wear, and surface integrity. (iv)Drilling operation can be performed to determine the output

responses such as F_d, R_a, cylindricity error, and circularity error. (v)AWJM can be tried as an alternative way to compare hole quality and surface integrity with traditional drilling methods.

Author contributions M.S, wrote the main manuscript text and supervised by K. P. The algorithms and computer programming functions are carried out by S.B and B. L. All authors checked the manuscript for its correctness and agreed for Publication.
Data availability No datasets were generated or analysed during the current study.
Declarations

Conflict of interest The authors declare no competing interests.
References

[1] F. Arriaga, X. Wang, G. Íñiguez-González, D. F. Llana, M. Esteban, and P. Niemz, 'Mechanical Properties of Wood: A Review', *Forests*, vol. 14, no. 6, p. 1202, Jun. 2023, doi: 10.3390/f14061202.

[2] Y. Mao, L. Hu, and Z. J. Ren, 'Engineesred wood for a sustainable future', *Matter*, vol. 5, no. 5, pp. 1326–1329, May 2022, doi: 10.1016/j.matt.2022.04.013.

[3] H. O. Dossou-Yovo, V. Kindomihou, and B. Sinsin, 'Ethnobotanical research of tree species used in wood carving in Southern Benin: Perspective for sustainable forest conservation', *Ethnobotany Research and Applications*, vol. 20, Oct. 2020, doi: 10.32859/era.20.29.1-10.

[4] D. Bamwesigye *et al.*, 'Charcoal and Wood Biomass Utilization in Uganda: The Sokcioeconomic and Environmental Dynamics and Implications', *Sustainability*, vol. 12, no. 20, p. 8337, Oct. 2020, doi: 10.3390/su12208337.

[5] J. . Burley, John. Youngquist, and Julian. Evans, *Encyclopedia of forest sciences*. Elsevier, 2004.

[6] M. C. Mistretta, F. P. La Mantia, V. Titone, B. Megna, L. Botta, and M. Morreale, 'Durability of Biodegradable Polymers for the Conservation of Cultural Heritage', *Front. Mater.*, vol. 6, Jun. 2019, doi: 10.3389/fmats.2019.00151.

[7] Z. Zhao, Z. Zhang, H. Wang, C. Li, L. Le, and M. Liu, ‘Functional wood-plastic composites: A review of research progress on flame retardancy, weather resistance and antimicrobial properties’, *Ind. Crops Prod.*, vol. 223, p. 120196, Jan. 2025, doi: 10.1016/j.indcrop.2024.120196.

[8] R. Bouza, C. Marco, M. Naffakh, L. Barral, and G. Ellis, ‘Effect of particle size and a processing aid on the crystallization and melting behavior of iPP/red pine wood flour composites’, *Compos. Part A Appl. Sci. Manuf.*, vol. 42, no. 8, pp. 935–949, Aug. 2011, doi: 10.1016/j.compositesa.2011.03.022.

[9] P. Manimaran *et al.*, ‘Extraction and characterization of natural lignocellulosic fibres from Typha angustata grass’, *Int. J. Biol. Macromol.*, vol. 222, pp. 1840–1851, Dec. 2022, doi: 10.1016/j.ijbiomac.2022.09.273.

[10] H. Ning, N. Lu, A. A. Hassen, K. Chawla, M. Selim, and S. Pillay, ‘A review of Long fibre thermoplastic (LFT) composites’, *International Materials Reviews*, vol. 65, no. 3, pp. 164–188, Apr. 2020, doi: 10.1080/09506608.2019.1585004.

[11] Q. Sun and B. Bai, ‘Application of modified rice straw/PP woodplastic composite material in landscape’, *ITM Web of Conferences*, vol. 47, p. 03028, Jun. 2022, doi: 10.1051/itmconf/20224703028.

[12] Y. Zhang, P. Xue, Y. Ding, M. Jia, J. Cai, and X. Jin, ‘Improvement of Mechanical Properties of Wood-Plastic Composite Floors Based on the Optimum Structural Design’, *Acta Mechanica Solida Sinica*, vol. 29, no. 4, pp. 444–454, Aug. 2016, doi: 10.1016/S0894-9166(16)30246-4.

[13] Y.-F. Shih, C.-W. Chang, T.-H. Hsu, and W.-Y. Dai, ‘Application of Sustainable Wood-Plastic Composites in Energy-Efficient Construction’, *Buildings*, vol. 14, no. 4, p. 958, Apr. 2024, doi: 10.3390/buildings14040958.

[14] J. Guo, H. Zhu, Y. Ma, L. Du, and J. Gao, ‘Application performance of bio-based plasticizer for PVC automotive interior material’, *Materials Testing*, vol. 65, no. 7, pp. 1097–1104, Jul. 2023, doi: 10.1515/mt-2022-0345.

[15] J. Korol, D. Burchart-Korol, and M. Pichlak, ‘Expansion of environmental impact assessment for eco-efficiency evaluation of biocomposites for industrial

application', *J. Clean. Prod.*, vol. 113, pp. 144–152, Feb. 2016, doi: 10.1016/j.jclepro.2015.11.101.

[16] G. KOWALUK, *Machining processes for wood-based composite materials*. Woodhead Publishing Limited, 2012.

[17] A. P. Singh, M. Sharma, and I. Singh, 'A review of modeling and control during drilling of fiber reinforced plastic composites', *Compos. B Eng.*, vol. 47, pp. 118–125, Apr. 2013, doi: 10.1016/j.compositesb.2012.10.038.

[18] L. M. P. Durão, M. F. S. F. de Moura, and A. T. Marques, 'Numerical simulation of the drilling process on carbon/epoxy composite laminates', *Compos. Part A Appl. Sci. Manuf.*, vol. 37, no. 9, pp. 1325–1333, Sep. 2006, doi: 10.1016/j.compositesa.2005.08.013.

[19] S. R. Karnik, V. N. Gaitonde, J. C. Rubio, A. E. Correia, A. M. Abrão, and J. P. Davim, 'Delamination analysis in high speed drilling of carbon fiber reinforced plastics (CFRP) using artificial neural network model', *Mater. Des.*, vol. 29, no. 9, pp. 1768–1776, Oct. 2008, doi: 10.1016/j.matdes.2008.03.014.

[20] U. Khashaba, 'DELAMINATION IN DRILLING GFR-THERMOSET COMPOSITES', *International Conference on Aerospace Sciences and Aviation Technology*, vol. 10, no. ASAT CONFERENCE, pp. 1–21, May 2003, doi: 10.21608/asat.2013.24453.

[21] P. Kayaroganam, V. Krishnan, E. Natarajan, S. Natarajan, and K. Muthusamy, 'Drilling Parameters Analysis on In-Situ Al/B4C/Mica Hybrid Composite and an Integrated Optimization Approach Using Fuzzy Model and Non-Dominated Sorting Genetic Algorithm', *Metals (Basel).*, vol. 11, no. 12, p. 2060, Dec. 2021, doi: 10.3390/met11122060.

[22] S. Prakash and K. Palanikumar, 'Modeling for prediction of surface roughness in drilling MDF panels using response surface methodology', *J. Compos. Mater.*, vol. 45, no. 16, pp. 1639–1646, Aug. 2011, doi: 10.1177/0021998310385026.

[23] M. Sundarapandiyan, K. Palanikumar, N. Senthilkumar, and B. Latha, 'Artificial intelligence-based optimization and response surface analysis of thrust force

and torque in drilling wood – thermoplastic composite (WPC) panels', *Wood Mater. Sci. Eng.*, pp. 1–19, Sep. 2025, doi: 10.1080/17480272.2025.2551740.

[24] B. Latha and V. S. Senthilkumar, 'Analysis of Thrust Force in Drilling Glass Fiber-Reinforced Plastic Composites Using Fuzzy Logic', *Materials and Manufacturing Processes*, vol. 24, no. 4, pp. 509–516, Feb. 2009, doi: 10.1080/10426910802714688.

[25] M. Slamani *et al.*, 'Investigating the impact of drill material on hole quality in jute/palm fiber reinforced hybrid composite drilling with uncertainty analysis', *Heliyon*, vol. 10, no. 17, p. e36925, Sep. 2024, doi: 10.1016/j.heliyon.2024.e36925.

[26] B. Bedelean, M. Ispas, and S. Răcășan, 'Optimizing Wood Composite Drilling with Artificial Neural Network and Response Surface Methodology', *Forests*, vol. 15, no. 9, p. 1600, Sep. 2024, doi: 10.3390/f15091600.

[27] S. Kumar, R. Das, and S. K. Parida, 'Experimental study on the quality of drilled holes in Sabai grass reinforced composites', *Mater. Today Proc.*, Mar. 2023, doi: 10.1016/j.matpr.2023.03.014.

[28] T. N. Valarmathi, K. Palanikumar, S. Sekar, and B. Latha, 'Investigation of the effect of process parameters on surface roughness in drilling of particleboard composite panels using adaptive neuro fuzzy inference system', *Materials and Manufacturing Processes*, vol. 35, no. 4, pp. 469–477, Mar. 2020, doi: 10.1080/10426914.2020.1711931.

[29] K. Palanikumar and T. N. Valarmathi, 'Experimental Investigation and Analysis on Thrust Force in Drilling of Wood Composite Medium Density Fiberboard Panels', *Exp. Tech.*, vol. 40, no. 1, pp. 391–400, Feb. 2016, doi: 10.1007/s40799-016-0044-6.

[30] A. Elhadi, S. Amroune, M. Slamani, M. Arslane, and M. Jawaid, 'Assessment and analysis of drilling-induced damage in jute/palm date fiber-reinforced polyester hybrid composite', *Biomass Convers. Biorefin.*, vol. 15, no. 3, pp. 4243–4258, Feb. 2025, doi: 10.1007/s13399-023-05251-0.

[31] K. Palanikumar and T. N. Valarmathi, ‘Experimental Investigation and Analysis on Thrust Force in Drilling of Wood Composite Medium Density Fiberboard Panels’, *Exp. Tech.*, vol. 40, no. 1, pp. 391–400, Feb. 2016, doi: 10.1007/s40799-016-0044-6.

[32] Ethem. Alpaydin, *Introduction to machine learning*. The MIT Press, 2020.

[33] Brown S, ‘Machine learning’, MIT Sloan management.

[34] J. A. Nichols, H. W. Herbert Chan, and M. A. B. Baker, ‘Machine learning: applications of artificial intelligence to imaging and diagnosis’, *Biophys. Rev.*, vol. 11, no. 1, pp. 111–118, Feb. 2019, doi: 10.1007/s12551-018-0449-9.

[35] Shaveta, ‘A review on machine learning’, *International Journal of Science and Research Archive*, vol. 9, no. 1, pp. 281–285, May 2023, doi: 10.30574/ijsra.2023.9.1.0410.

[36] I. H. Sarker, ‘Machine Learning: Algorithms, Real-World Applications and Research Directions’, *SN Comput. Sci.*, vol. 2, no. 3, p. 160, May 2021, doi: 10.1007/s42979-021-00592-x.

[37] R. P. França, A. C. Borges Monteiro, R. Arthur, and Y. Iano, ‘An overview of deep learning in big data, image, and signal processing in the modern digital age’, in *Trends in Deep Learning Methodologies*, Elsevier, 2021, pp. 63–87. doi: 10.1016/B978-0-12-822226-3.00003-9.

[38] ReneY. Choi, Aaron S. Coyner, Jayashree Kalpathy-Cramer, Michael F. Chiang, and J. Peter Campbell, ‘Introduction to Machine Learning, Neural Networks, andDeepLearning’, *Transl. Vis. Sci. Technol.*, vol. 19, no. 14, pp. 1–12, Feb. 2020.

[39] J. L. Uc Castillo, A. E. Marín Celestino, D. A. Martínez Cruz, J. Tuxpan Vargas, J. A. Ramos Leal, and J. Morán Ramírez, ‘A systematic review of Machine Learning and Deep Learning approaches in Mexico: challenges and opportunities’, *Front. Artif. Intell.*, vol. 7, Jan. 2025, doi: 10.3389/frai.2024.1479855.

[40] M. M. Taye, ‘Understanding of Machine Learning with Deep Learning: Architectures, Workflow, Applications and Future Directions’, *Computers*, vol. 12, no. 5, p. 91, Apr. 2023, doi: 10.3390/computers12050091.

[41] R. Pugliese, S. Regondi, and R. Marini, ‘Machine learning-based approach: global trends, research directions, and regulatory standpoints’, *Data Science and Management*, vol. 4, pp. 19–29, Dec. 2021, doi: 10.1016/j.dsm.2021.12.002.

[42] S. Sah, ‘Machine Learning: A Review of Learning Types’, Jul. 11, 2020. doi: 10.20944/preprints202007.0230.v1.

[43] J. Jovel and R. Greiner, ‘An Introduction to Machine Learning Approaches for Biomedical Research’, *Front. Med. (Lausanne).*, vol. 8, Dec. 2021, doi: 10.3389/fmed.2021.771607.

[44] C. Janiesch, P. Zschech, and K. Heinrich, ‘Machine learning and deep learning’, *Electronic Markets*, vol. 31, no. 3, pp. 685–695, Sep. 2021, doi: 10.1007/s12525-021-00475-2.

[45] E. Barbierato and A. Gatti, ‘The Challenges of Machine Learning: A Critical Review’, *Electronics (Basel).*, vol. 13, no. 2, p. 416, Jan. 2024, doi: 10.3390/electronics13020416.

[46] S. Badillo *et al.*, ‘An Introduction to Machine Learning’, *Clin. Pharmacol. Ther.*, vol. 107, no. 4, pp. 871–885, Apr. 2020, doi: 10.1002/cpt.1796.

[47] I. C. Udousoro, ‘Machine Learning: A Review’, *Semiconductor Science and Information Devices*, vol. 2, no. 2, pp. 5–14, Nov. 2020, doi: 10.30564/ssid.v2i2.1931.

[48] H. Gao *et al.*, ‘Machine learning in business and finance: a literature review and research opportunities’, *Financial Innovation*, vol. 10, no. 1, p. 86, Sep. 2024, doi: 10.1186/s40854-024-00629-z.

[49] Z.-H. Zhou, ‘Open-environment machine learning’, *Natl. Sci. Rev.*, vol. 9, no. 8, Aug. 2022, doi: 10.1093/nsr/nwac123.

[50] S. Geetha Gowri, R.Devi, and D K Sethuraman, ‘MACHINE LEARNING’, *International Journal of Research and Analytical Reviews*, vol. 6, no. 2, pp. 197–208, Jun. 2019.

[51] R. Panchendrarajan and A. Zubiaga, ‘Synergizing machine learning & symbolic methods: A survey on hybrid approaches to natural language processing’, *Expert Syst. Appl.*, vol. 251, p. 124097, Oct. 2024, doi: 10.1016/j.eswa.2024.124097.

[52] P. Hitzler, A. Eberhart, M. Ebrahimi, M. K. Sarker, and L. Zhou, ‘Neuro-symbolic approaches in artificial intelligence’, *Natl. Sci. Rev.*, vol. 9, no. 6, Jun. 2022, doi: 10.1093/nsr/nwac035.

[53] X. Hua *et al.*, ‘Prediction of Thermomechanical Behavior of Wood–Plastic Composites Using Machine Learning Models: Emphasis on Extreme Learning Machine’, *Polymers (Basel).*, vol. 17, no. 13, p. 1852, Jul. 2025, doi: 10.3390/polym17131852.

[54] A. K P, U. Vignesh Nayak, K. M. Pranesh Rao, S. H T, V. L. Neelakantha, and S. C M, ‘Optimization of drilling parameters to minimize delamination in CNT-filled GFRP composites using machine learning’, *Applications in Engineering Science*, vol. 23, p. 100257, Sep. 2025, doi: 10.1016/j.apples.2025.100257.

[55] S. Zhang, W. Wang, T. Zhang, Y. Xiong, B. Huang, and R. Jiang, ‘Evaluation of hole quality in drilling CF/BMI composite via machine learning: Multi-defects analysis and fatigue life prediction’, *Thin-Walled Structures*, vol. 212, p. 113189, Jul. 2025, doi: 10.1016/j.tws.2025.113189.

[56] K. Biruk-Urban, P. Bere, and J. Józwik, ‘Machine Learning Models in Drilling of Different Types of Glass-Fiber-Reinforced Polymer Composites’, *Polymers (Basel).*, vol. 15, no. 23, p. 4609, Dec. 2023, doi: 10.3390/polym15234609.

[57] A. Akdulum and Y. Kayir, ‘Prediction of thrust force in indexable drilling of aluminum alloys with machine learning algorithms’, *Measurement*, vol. 222, p. 113655, Nov. 2023, doi: 10.1016/j.measurement.2023.113655.

[58] H. Dedeakayoğulları, A. Kaçal, and K. Keser, ‘Modeling and prediction of surface roughness at the drilling of SLM-Ti6Al4V parts manufactured with pre-

hole with optimized ANN and ANFIS', *Measurement*, vol. 203, p. 112029, Nov. 2022, doi: 10.1016/j.measurement.2022.112029.

[59] S. K. H. Lee, P. G. Mongan, A. Farhadi, E. P. Hinchy, N. P. O'Dowd, and C. T. McCarthy, 'In-situ evaluation of hole quality and cutting tool condition in robotic drilling of composite materials using machine learning', *J. Intell. Manuf.*, Jan. 2025, doi: 10.1007/s10845-024-02528-7.

[60] Koosha Sharifani and Mahyar Amini, 'Machine Learning and Deep Learning: A Review of Methods and Applications', *World Information Technology and Engineering*, vol. 10, no. 07, pp. 3897–3904, Mar. 2021.

[61] K. Kolasa, B. Admassu, M. Hołownia-Voloskova, K. J. Kędzior, J.-E. Poirrier, and S. Perni, 'Systematic reviews of machine learning in healthcare: a literature review', *Expert Rev. Pharmacoecon. Outcomes Res.*, vol. 24, no. 1, pp. 63–115, Jan. 2024, doi: 10.1080/14737167.2023.2279107.

[62] K. Szwajka, J. Zielińska-Szwajka, and T. Trzepiecinski, 'Experimental Study on Drilling MDF with Tools Coated with TiAlN and ZrN', *Materials*, vol. 12, no. 3, p. 386, Jan. 2019, doi: 10.3390/ma12030386.

[63] K. Palanikumar and T. N. Valarmathi, 'Experimental Investigation and Analysis on Thrust Force in Drilling of Wood Composite Medium Density Fiberboard Panels', *Exp. Tech.*, vol. 40, no. 1, pp. 391–400, Feb. 2016, doi: 10.1007/s40799-016-0044-6.

[64] T. Raja, Y. Devarajan, G. Dhanraj, S. Pandiaraj, M. Rahaman, and M. Thiruvengadam, 'Delamination analysis of drilling parameters on neem/banyan fiber–reinforced sawdust particulates hybrid polymer composite', *Biomass Convers. Biorefin.*, vol. 14, no. 9, pp. 10747–10757, May 2024, doi: 10.1007/s13399-023-04951-x.

[65] M. Sundarapandiyan, K. Palanikumar, N. Senthilkumar, and B. Latha, 'Artificial intelligence-based optimization and response surface analysis of thrust force and torque in drilling wood – thermoplastic composite (WPC) panels', *Wood Mater. Sci. Eng.*, pp. 1–19, Sep. 2025, doi: 10.1080/17480272.2025.2551740.

[66] T. N. Valarmathi, K. Palanikumar, and B. Latha, ‘Measurement and analysis of thrust force in drilling of particle board (PB) composite panels’, *Measurement*, vol. 46, no. 3, pp. 1220–1230, Apr. 2013, doi: 10.1016/j.measurement.2012.11.024.

[67] T. Raja, Y. Devarajan, G. Dhanraj, S. Pandiaraj, M. Rahaman, and M. Thiruvengadam, ‘Delamination analysis of drilling parameters on neem/banyan fiber–reinforced sawdust particulates hybrid polymer composite’, *Biomass Convers. Biorefin.*, vol. 14, no. 9, pp. 10747–10757, May 2024, doi: 10.1007/s13399-023-04951-x.

[68] M. Sundarapandiyan, K. Palanikumar, N. Senthilkumar, and B. Latha, ‘Artificial intelligence-based optimization and response surface analysis of thrust force and torque in drilling wood – thermoplastic composite (WPC) panels’, *Wood Mater. Sci. Eng.*, pp. 1–19, Sep. 2025, doi: 10.1080/17480272.2025.2551740.